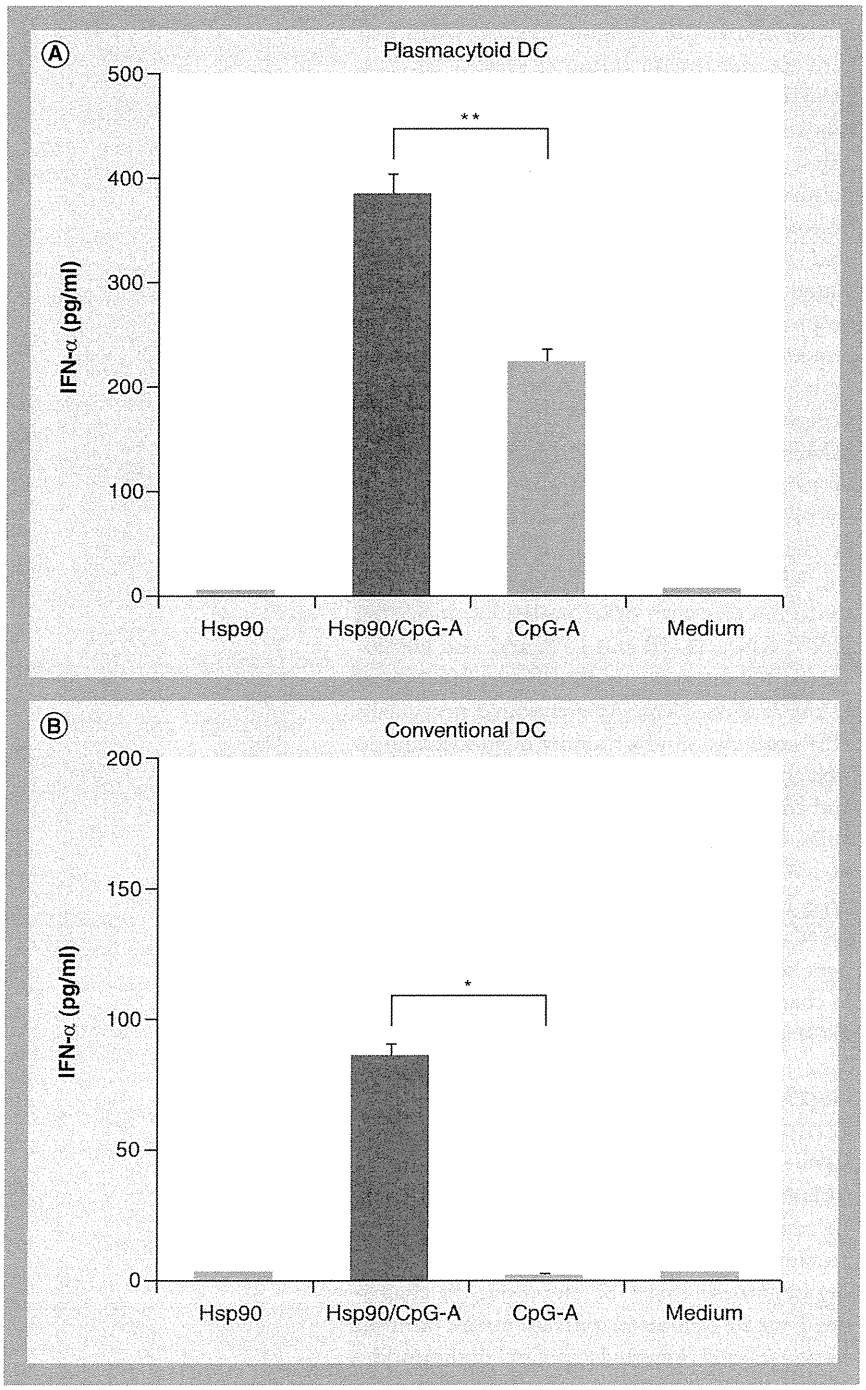

Figure 1. Hsp90–CpG-A complexes enhance induction of IFN-α by murine dendritic cells. (A) Hsp90–CpG-A complexes induce IFN-α production by plasmacytoid DCs to a level twofold higher than that induced by CpG-A alone. **(B)** Conventional DCs produce IFN-α when stimulated with Hsp90-CpG-A complex but not when stimulated with CpG-A alone. Hsp90 alone does not have any effect on IFN-α production. Data are presented as means + standard error of the mean of triplicate wells.
*$p < 0.0005$, **$p < 0.001$; paired student t-test.
DC: Dentric cell.

observed IFN-α production was shown to be TLR9-dependent. We found that Hsp90-chaperoned CpG-A was localized and retained within static early endosomes for longer periods in cDCs, thereby eliciting TLR9 signaling for IFN-α production, but not inflammatory cytokines such as IL-6 and TNF-α. By contrast, CpG-A alone moved into late endosomes and lysosomes within cDCs. Interestingly, not only CpG-A but also CpG-B could stimulate the TLR9 signaling within static early endosomes, resulting in the production of IFN-α. Thus, extracellular Hsp90 has the ability to direct associated CpGs into static early endosomes, leading to interferon regulatory factor 7 activation and IFN-α production.

Why, however, are DNA–Hsp90 complexes retained in early endosomes but not in late endosomes or lysosomes in DCs? We found that endocytosed CpG-A–Hsp90 complexes were selectively transferred into $Rab5^+$, early endosomal antigen (EEA)-1^+ static early endosomes. Very recently, Lakadamyali *et al.* have shown that early endosomes are comprised of two distinct populations, a dynamic population that is highly mobile on microtubules and matures rapidly toward the late endosome and a static population that matures much more slowly [63]. Cargos destined for degradation, including low-density lipoprotein, EGF and influenza virus, are internalized and targeted to the $Rab5^+$, $EEA1^-$ dynamic population of early endosomes, thereafter trafficking to $Rab7^+$ late endosomes. By contrast, the recycling transferrin is delivered to $Rab5^+$, $EEA1^+$ static early endosomes, followed by translocation to $Rab11^+$ recycling endosomes. They also found that cargos trafficked into these static early endosomes were retained for longer periods and not translocated into late endosomes and lysosomes. Thus, our observation that the CpG-A–Hsp90 complex was retained in static early endosomes, leading to sustained activation of DCs and IFN-α production, is consistent with their findings (FIGURE 2).

Hsp90 as a possible accelerator for autoimmune diseases

pDCs normally do not respond to self-DNA, which may reflect the fact that viral/bacterial DNA sequences contain multiple CpG nucleotides that bind and activate TLR9, whereas mammalian self-DNA contains fewer such motifs, which are most likely masked by methylation. Recent evidence, however, suggests that self-DNA has the potential to trigger TLR9 but may fail to do so because it fails to access the TLR9-containing endolysosomal compartments. One of the mechanisms to which this effect is attributed is the fact that DNase easily and rapidly breaks down extracellular DNA, thereby hampering self-DNA localization into

endocytic compartments. The importance of this mechanism in preventing autoimmune responses has been shown by the fact that mice deficient in DNase II develop systemic lupus erythematosus (SLE)-like syndrome [64]. Recently, it has been demonstrated that pDCs do sense and respond to self-DNA in human autoimmune diseases. Therefore, we examined whether Hsp90 targets self-DNA into static early endosomes, resulting in IFN-α production by human pDCs [60]. Upon Hsp90-mediated enforced endosomal translocation, both human self-DNA and CpG-ODN could activate DCs via TLR9 to produce IFN-α. Previous studies have demonstrated the presence of autoantibodies to Hsp90 [65,66] and enhanced expression of Hsp90 in peripheral blood mononuclear cells of patients with active SLE [67,68], suggesting a role of Hsp90 in the pathogenesis. In addition, Hsp90 has been shown to localize both in the cytoplasm and nucleus [69]. Moreover, under stressful conditions, it has been shown that cytosolic Hsp90 translocates to the nucleus [70]. This suggests that Hsp90 may bind self-DNA within the nucleus. When cells undergo necrosis, self-DNA associated with endogenous Hsp90 could be released into the extracellular space and might trigger IFN-α production by pDCs. Our findings support the idea that Hsp90, an endogenous danger signal molecule found in sera of SLE patients, might be the key mediator of pDC activation in SLE. Thus, Hsp90 may activate innate immunity to self-DNA by forming a complex with self-DNA that is delivered to and retained within early endocytic compartments of pDCs to trigger TLR9 and induce IFN production. Thus, we determined a fundamental mechanism by which pDCs sense and respond to self-DNA coupled with Hsp90. Our data suggest that, through this pathway, pDCs drive autoimmunity in autoimmune diseases. Several host factors other than Hsp90 that can convert self-DNA into a trigger of DC activation have been reported. Endogenous cationic antimicrobial peptide LL37 (also known as CAMP) [71], autoantibodies [72] and HMGB1 [59] have been demonstrated to do so by forming a complex with host-derived DNA. Together, these findings indicate that the ability of some of DAMPs to convert self-DNA into a trigger of high levels of IFN-α production depends on the capacity of DAMPs to concentrate and retain DNA in static early endosomes, thus enabling the selective and sustained activation of early endosomal TLR9.

Cross-presentation mediated by HSP: pivotal role of Hsp90

HSPs inherently act as molecular chaperones, and in our opinion, from an immunological point of view, the most characteristic finding is that HSPs can bind antigenic peptides within cells. Therefore, immunization with a HSP–antigenic

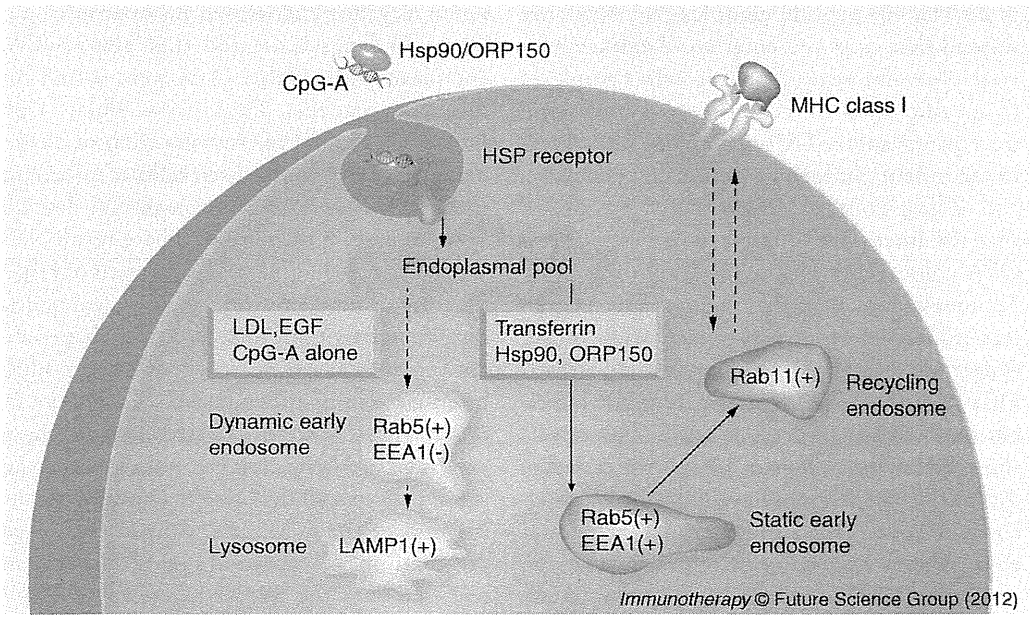

Figure 2. Extracellular Hsp90/ORP150 targets chaperoned molecules into static early endosomes. Early endosomes are comprised of static early endosomes (Rab5$^+$ and EEA-1$^+$) and dynamic early endosomes (Rab5$^+$ and EEA-1$^-$). Hsp90/ORP150-antigen or Hsp90–CpG-A complexes are preferentially targeted and retained in static early endosomes of DCs, leading to efficient antigen cross-presentation as well as sustained activation of Toll-like receptor 9 and IFN-α production.
Hsp: Heat-shock protein; LDL: Low-density lipoprotein.

peptide complex elicits antigen-specific cytotoxic T-cell responses. Therefore, extracellular HSP can deliver associated antigens into the MHC class I presentation pathway of antigen-presenting cells, a process called cross-presentation, thus inducing antigen-specific $CD8^+$ T-cell responses. However, the underlying mechanism for introduction of an exogenous antigen into a cross-presentation pathway remains unclear, and the precise mechanism for intracellular antigen translocation and the processing pathway have not been fully elucidated. Recent evidence indicates that exogenous antigens can be processed through at least two distinct pathways, one involving access of exogenous antigens to the classical MHC class I loading pathway (TAP-dependent) and the other involving unconventional post-Golgi loading of MHC class I molecules in endocytic compartments (TAP-independent) [73]. One or both of these pathways can contribute to cross-presentation depending on the source of exogenous antigens such as soluble proteins, immune complexes or peptides chaperoned by HSPs.

We first demonstrated that extracellular Hsp90-peptide complexes generated *in vitro* were efficiently cross-presented by DCs and recognized by peptide-specific CTLs via a TAP-independent 'endosome-recycling' pathway because DCs derived from TAP-knockout mice were fully functional in cross-presentation of an Hsp90–peptide complex [74]. Next, we showed that cross-presentation of extracellular Hsp90–ovalbumin (OVA) protein complexes to specific $CD8^+$ T cells involved both classical proteasome–TAP-dependent and TAP-independent endosome-recycling pathways [75]. Using confocal microscopy, we found that the internalized extracellular Hsp90 and OVA colocalized with cytosolic proteasomes. To investigate whether endogenous Hsp90 was responsible for cross-presentation of the exogenous Hsp90–OVA complex, we treated DCs with the Hsp90-specific inhibitor radicicol in a cross-presentation assay. The results showed that treatment of DCs with radicicol did not affect the cross-presentation of exogenous Hsp90-OVA, suggesting that endogenous Hsp90 might not be responsible for the exogenous Hsp90-mediated cross-presentation. Strikingly, when an anti-Hsp90 monoclonal antibody was introduced into DCs, the colocalization of internalized Hsp90-chaperoned OVA and proteasomes was abolished, resulting in inhibition of TAP-dependent cross-presentation of OVA. Thus, extracellular Hsp90 may play a pivotal role in the translocation of chaperoned antigens for proteasomal degradation in the cytosol. By contrast, a high concentration of soluble OVA (200 mg/ml) was cross-presented by DCs, although the cross-presentation was considerably less efficient than that of a Hsp90–OVA complex (20 μg/ml of OVA). Interestingly, this cross-presentation was radicicol-sensitive, indicating that endogenous Hsp90 played an important role in the cross-presentation of exogenous OVA. Udono *et al.* have elegantly demonstrated that endogenous Hsp90α was required for cross-presentation of exogenous OVA using DCs derived from Hsp90α-knockout mice [76]. Their findings also suggest that endogenous Hsp90, as well as exogenous Hsp90, might help the exogenous Hsp90–OVA complex translocate into cytosol at the cytosolic face for cross-presentation (FIGURE 3). By contrast, OVA chaperoned by Hsp90 was not presented by MHC class II molecules *in vitro* or *in vivo*, although the antigen was exogenously loaded onto DCs. To confirm these observations, we investigated the destination of Hsp90–OVA complexes and soluble OVA after its uptake in DCs, using confocal laser microscopy. Hsp90-chaperoned OVA was observed to colocalize with early endosomes, recycling endosomes, and proteasomes but not lysosomes. By contrast, soluble OVA was detected in early endosomes to lysosomes but not in recycling endosomes, ER or proteasomes. These findings indicated that Hsp90–OVA complexes and soluble OVA were sorted into different organelles. Thus, extracellular Hsp90 might be essential for translocation of chaperoned antigens from the extracellular milieu into the cytosol, resulting in proteasomal degradation for cross-presentation. These results have revealed a novel mode of involvement of Hsp90 in antigen presentation by DCs: exogenous Hsp90 preferentially introduces the chaperoned antigen into the MHC class I pathway, resulting in efficient cross-presentation. Since there is a classical paradigm that extracellular antigens are presented by MHC class II molecules, it seemed significant to find that Hsp90 changed the destination of the associated antigen on antigen presentation. Calderwood's group has recently reported that the SREC-1 acts as an Hsp90 receptor for cross-presentation on DCs [77]. As described previously, Lakadamyali *et al.* demonstrated that early endosomes are comprised of two distinct populations: a dynamic population that matures rapidly toward the late endosome and lysosome, and a static early endosome that

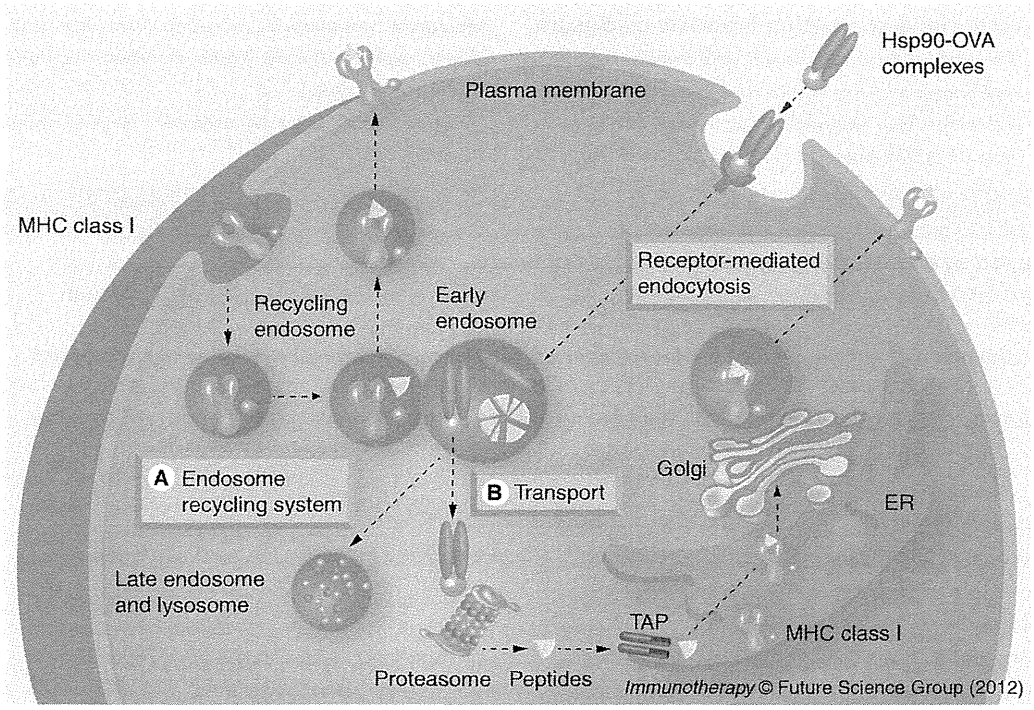

Figure 3. Pathway for Hsp90-antigen complex-mediated cross-presentation by DCs.
Internalized Hsp90-antigen complexes through receptor-mediated endocytosis follow two distinct MHC class I pathways. **(A)** Internalized antigens chaperoned by Hsp90 are processed by endosomal peptidases such as cathepsin S and are loaded in the endocytic pathway onto MHC class I molecules that are recycled from the plasma membrane (TAP-independent pathway). **(B)** Alternatively, internalized Hsp90-antigen complexes are translocated to the cytosol and are degraded by the proteasome. Resultant peptides are imported into the ER in a TAP-dependent fashion and are loaded onto newly synthesized MHC class I molecules.
ER: Endoplasmic reticulum; OVA: Ovalbumin.

matures much more slowly [63]. Interestingly, Burgdorf *et al.* demonstrated that a mannose receptor introduces exogenous OVA specifically into an EEA-1$^+$, Rab5$^+$ static early endosomal compartment for subsequent cross-presentation [78,79]. These observations are consistent with dynamics of extracellular Hsp90 demonstrated by us. By contrast, OVA endocytosed by a SR did not colocalize with EEA-1; instead, it colocalized with LAMP-1 in the lysosome as shown here, leading to presentation in the context of MHC class II molecules. Thus, we expect that Hsp90-specific receptors such as SREC-1 might introduce the Hsp90–OVA complex into the static early endosome for cross-presentation. Furthermore, we have recently shown that an ER-resident Hsp70 family member, oxygen-regulated protein 150 (ORP150), localized to static early endosomes after endocytosis, leading to antigen cross-presentation when pulsed onto DCs [80]. These CTLs induced by immunization with Hsp90/ORP150 peptide complexes could inhibit established tumor growth, indicating that Hsp90/ORP150 peptide complexes act as cancer vaccines. Importantly, the Hsp90/ORP150-mediated cross-presentation pathway for exogenous peptides has been shown to be an endosome-recycling pathway, not a conventional TAP-dependent pathway. Targeting static early endosomes is the key feature of Hsp90/ORP150 for inducing innate as well as adaptive immune responses. These findings provide a rationale for the development of Hsp90-based vaccination strategies for cancer as well as viral immunity.

Future perspective

Can all HSPs target chaperoned molecules to static early endosomes? It has been shown that Hsp90 and ORP150 could be targeted to static early endosomes after endocytosis, leading to antigen cross-presentation when pulsed onto DCs. Whether this is the case for other HSPs, however, remains to be determined. More importantly, the HSP receptor responsible for targeting to static early endosomes should be clarified. Elucidation of the molecular basis for sorting HSPs to static endosomes will also be necessary to establish HSP-based cancer vaccines.

Financial & competing interests disclosure

The authors have no relevant affiliations or financial involvement with any organization or entity with a financial interest in or financial conflict with the subject matter or materials discussed in the manuscript. This includes employment, consultancies, honoraria, stock ownership or options, expert testimony, grants or patents received or pending, or royalties.

No writing assistance was utilized in the production of this manuscript.

Executive summary

Heat-shock proteins are key players in orchestrating innate & adaptive immunity

- Extracellular heat-shock proteins (HSPs) behave as endogenous danger signals for activation of innate immune responses through binding to Toll-like receptors (TLRs).
- Extracellular HSPs can bind innate ligands and augment innate immune responses through spatiotemporal regulation of chaperoned ligands.
- Extracellular HSP–antigen complexes are cross-presented by antigen-presenting cells via both a TAP-independent endocytic pathway and a TAP-dependent pathway.

HSP release & HSP receptors

- HSPs are released from cells by passive and active mechanisms in response to several kinds of stress.
- TLRs and scavenger receptors have been identified as receptors for HSPs expressed on antigen-presenting cells such as dendritic cells (DCs).

Spatiotemporal regulation of HSPs

- Extracellular Hsp90/ORP150 is targeted to static early endosomes within DCs.
- Extracellular Hsp90–self-DNA/CpG-A complex can stimulate IFN-α production by DCs via spatiotemporal regulation.
- Both extracellular Hsp90 and endogenous Hsp90 may be involved in translocation of exogenous antigen from the endosome to the cytosol for degradation by proteasome, leading to antigen cross-presentation.

Conclusion

- HSPs can link innate and adaptive immune responses, leading to amplified immune responses.
- HSPs are attractive candidates for vaccine development due to their ability to target DCs and to induce specific cytotoxic T cells without the need for an adjuvant.
- Elucidation of the molecular basis for sorting HSPs to static endosomes should lead to the establishment of HSP-based cancer vaccines.

References

Papers of special note have been highlighted as:
▪ of interest
▪▪ of considerable interest

1 Richter K, Haslbeck M, Buchner J. The heat shock response: life on the verge of death. *Mol. Cell* 40(2), 253–266 (2010).

2 Calderwood SK, Mambula SS, Gray PJ Jr, Theriault JR. Extracellular heat shock proteins in cell signaling. *FEBS Lett.* 581(19), 3689–3694 (2007).

3 Udono H, Levey DL, Srivastava PK. Cellular requirements for tumor-specific immunity elicited by heat shock proteins: tumor rejection antigen gp96 primes $CD8^+$ T cells *in vivo*. *Proc. Natl Acad. Sci. USA* 91(8), 3077–3081 (1994).

4 Srivastava P. Interaction of heat shock proteins with peptides and antigen presenting cells: chaperoning of the innate and adaptive immune responses. *Annu. Rev. Immunol.* 20, 395–425 (2002).

▪▪ **Overview of heat-shock protein (Hsp)-mediated immune responses.**

5 Udono H, Srivastava PK. Heat shock protein 70-associated peptides elicit specific cancer immunity. *J. Exp. Med.* 178(4), 1391–1396 (1993).

6 Udono H, Srivastava PK. Comparison of tumor-specific immunogenicities of stress-induced proteins gp96, Hsp90, and Hsp70. *J. Immunol.* 152(11), 5398–5403 (1994).

7 Noessner E, Gastpar R, Milani V *et al.* Tumor-derived heat shock protein 70 peptide complexes are cross-presented by human dendritic cells. *J. Immunol.* 169(10), 5424–5432 (2002).

8 Mambula SS, Calderwood SK. Heat shock protein 70 is secreted from tumor cells by a nonclassical pathway involving lysosomal endosomes. *J. Immunol.* 177(11), 7849–7857 (2006).

▪ **Demonstrates the unique mechanism for the release of Hsp70 from tumor cells.**

9 Asea A, Kraeft SK, Kurt-Jones EA *et al.* Hsp70 stimulates cytokine production through a CD14-dependent pathway, demonstrating its dual role as a chaperone and cytokine. *Nat. Med.* 6(4), 435–442 (2000).

10 Asea A, Rehli M, Kabingu E *et al.* Novel signal transduction pathway utilized by extracellular Hsp70: role of Toll-like receptor (TLR) 2 and TLR4. *J. Biol. Chem.* 277(17), 15028–15034 (2002).

11 Asea A. Initiation of the immune response by extracellular Hsp72: chaperokine activity of Hsp72. *Curr. Immunol. Rev.* 2(3), 209–215 (2006).

12 Norbury CC, Basta S, Donohue KB *et al.* $CD8^+$ T cell cross-priming via transfer of proteasome substrates. *Science* 304(5675), 1318–1321 (2004).

13 Sato A, Tamura Y, Sato N *et al.* Melanoma-targeted chemo-thermo-immuno (CTI)-therapy using *N*-propionyl-4-*S*-cysteaminylphenol-magnetite nanoparticles elicits CTL response via heat shock protein-peptide complex release. *Cancer Sci.* 101(9), 1939–1946 (2010).

14 Binder RJ, Han DK, Srivastava PK. CD91: a receptor for heat shock protein gp96. *Nat. Immunol.* 1(2), 151–155 (2000).

15 Calderwood SK, Mambula SS, Gray PJ Jr, Theriault JR. Extracellular heat shock proteins in cell signaling. *FEBS Lett.* 581(19), 3689–3694 (2007).

▪▪ **Overview of HSP receptors and their significance in immunity.**

16 Asea A, Kabingu E, Stevenson MA, Calderwood SK. Hsp70 peptidembearing and peptide-negative preparations act as

chaperokines. *Cell Stress Chaperones* 5(5), 425–431 (2000).

17 Basu S, Binder RJ, Suto R, Anderson KM, Srivastava PK. Necrotic but not apoptotic cell death releases heat shock proteins, which deliver a partial maturation signal to dendritic cells and activate the NF-κB pathway. *Int. Immunol.* 12(11), 1539–1546 (2000).

18 Vabulas RM, Ahmad-Nejad P, Ghose S, Kirschning CJ, Issels RD, Wagner H. Hsp70 as endogenous stimulus of the Toll/interleukin-1 receptor signal pathway. *J. Biol. Chem.* 277(17), 15107–15112 (2002).

19 Javid B, Macary PA, Lehner PJ. Structure and function: heat shock proteins and adaptive immunity. *J. Immunol.* 179(4), 2035–2040 (2007).

20 Wheeler DS, Dunsmore KE, Denenberg AG, Muething L, Poynter SE, Wong HR. Biological activity of truncated C-terminus human heat shock protein 72. *Immunol. Lett.* 135(1–2), 173–179 (2011).

21 Theriault JR, Mambula SS, Sawamura T, Stevenson MA, Calderwood SK. Extracellular Hsp70 binding to surface receptors present on antigen presenting cells and endothelial/epithelial cells. *FEBS Lett.* 579(9), 1951–1960 (2005).

22 Shi Y, Evans JE, Rock KL. Molecular identification of a danger signal that alerts the immune system to dying cells. *Nature* 425(6957), 516–521 (2003).

23 Basu S, Binder RJ, Ramalingam T, Srivastava PK. CD91 is a common receptor for heat shock proteins gp96, Hsp90, Hsp70, and calreticulin. *Immunity* 14(3), 303–313 (2001).

24 Delneste Y, Magistrelli G, Gauchat J *et al.* Involvement of LOX-1 in dendritic cell-mediated antigen cross-presentation. *Immunity* 17(3), 353–362 (2002).

25 Theriault JR, Adachi H, Calderwood SK. Role of scavenger receptors in the binding and internalization of heat shock protein 70. *J. Immunol.* 177(12), 8604–8611 (2006).

26 Berwin B, Hart JP, Rice S *et al.* Scavenger receptor-A mediates gp96/GRP94 and calreticulin internalization by antigen-presenting cells. *EMBO J.* 22(22), 6127–6136 (2003).

27 Berwin B, Delneste Y, Lovingood RV, Post SR, Pizzo SV. SREC-I, a type F scavenger receptor, is an endocytic receptor for calreticulin. *J. Biol. Chem.* 279(49), 51250–51257 (2004).

28 Wang XY, Facciponte J, Chen X, Subjeck JR, Repasky EA. Scavenger receptor-A negatively regulates antitumor immunity. *Cancer Res.* 67(10), 4996–5002 (2007).

29 Berwin B, Reed RC, Nicchitta CV. Virally induced lytic cell death elicits the release of immunogenic GRP94/gp96. *J. Biol. Chem.* 276(24), 21083–21088 (2001).

30 Barreto A, Gonzalez JM, Kabingu E, Asea A, Fiorentino S. Stress-induced release of HSC70 from human tumors. *Cell. Immunol.* 222(2), 97–104 (2003).

31 Gastpar R, Gehrmann M, Bausero MA *et al.* Heat shock protein 70 surface-positive tumor exosomes stimulate migratory and cytolytic activity of natural killer cells. *Cancer Res.* 65(12), 5238–5247 (2005).

32 Bausero MA, Gastpar R, Multhoff G, Asea A. Alternative mechanism by which IFN-γ enhances tumor recognition: active release of heat shock protein 72. *J. Immunol.* 175(5), 2900–2912 (2005).

33 Johnson JD, Campisi J, Sharkey CM, Kennedy SL, Nickerson M, Fleshner M. Adrenergic receptors mediate stress-induced elevations in extracellular Hsp72. *J. Appl. Physiol.* 99(5), 1789–1795 (2005).

34 Vega VL, Rodriguez-Silva M, Frey T *et al.* Hsp70 translocates into the plasma membrane after stress and is released into the extracellular environment in a membrane-associated form that activates macrophages. *J. Immunol.* 180(6), 4299–4307 (2008).

35 De Maio A. Extracellular heat shock proteins, cellular export vesicles, and the stress observation system: a form of communication during injury, infection, and cell damage. It is never known how far a controversial finding will go! Dedicated to Ferruccio Ritossa. *Cell Stress Chaperones* 16(3), 235–249 (2011).

▪▪ **Overview of the mechanism of HSP release into extracellular milieu and its impact on immune responses.**

36 Matzinger P. The danger model: a renewed sense of self. *Science* 296(5566), 301–305 (2002).

37 Vabulas RM, Ahmad-Nejad P, Ghose S, Kirschning CJ, Issels RD, Wagner H. Hsp70 as endogenous stimulus of the Toll/interleukin-1 receptor signal pathway. *J. Biol. Chem.* 277(17), 15107–15112 (2002).

38 Chen X, Tao Q, Yu H, Zhang L, Cao X. Tumor cell membrane-bound heat shock protein 70 elicits antitumor immunity. *Immunol. Lett.* 84(2), 81–87 (2002).

39 Panjwani NN, Popova L, Srivastava PK. Heat shock proteins gp96 and Hsp70 activate the release of nitric oxide by APCs. *J. Immunol.* 168(6), 2997–3003 (2002).

40 Manjili MH, Park J, Facciponte JG, Subjeck JR. Hsp110 induces "danger signals" upon interaction with antigen presenting cells and mouse mammary carcinoma. *Immunobiology* 210(5), 295–303 (2005).

41 Basu S, Binder RJ, Suto R, Anderson KM, Srivastava PK. Necrotic but not apoptotic cell death releases heat shock proteins, which deliver a partial maturation signal to dendritic cells and activate the NF-κB pathway. *Int. Immunol.* 12(11), 1539–1546 (2000).

42 Chen T, Guo J, Han C, Yang M, Cao X. Heat shock protein 70, released from heat-stressed tumor cells, initiates antitumor immunity by inducing tumor cell chemokine production and activating dendritic cells via TLR4 pathway. *J. Immunol.* 182(3), 1449–1459 (2009).

43 Wallin RP, Lundqvist A, More SH, Von Bonin A, Kiessling R, Ljunggren HG. Heat-shock proteins as activators of the innate immune system. *Trends Immunol.* 23(3), 130–135 (2002).

44 Habich C, Kempe K, Van Der Zee R *et al.* Heat shock protein 60: specific binding of lipopolysaccharide. *J. Immunol.* 174(3), 1298–1305 (2005).

45 Reed RC, Berwin B, Baker JP, Nicchitta CV. GRP94/gp96 elicits ERK activation in murine macrophages. A role for endotoxin contamination in NF-κB activation and nitric oxide production. *J. Biol. Chem.* 278(34), 31853–31860 (2003).

46 Warger T, Hilf N, Rechtsteiner G *et al.* Interaction of TLR2 and TLR4 ligands with the N-terminal domain of Gp96 amplifies innate and adaptive immune responses. *J. Biol. Chem.* 281(32), 22545–22553 (2006).

47 Zheng H, Dai J, Stoilova D, Li Z. Cell surface targeting of heat shock protein gp96 induces dendritic cell maturation and antitumor immunity. *J. Immunol.* 167(12), 6731–6735 (2001).

48 Liu B, Dai J, Zheng H, Stoilova D, Sun S, Li Z. Cell surface expression of an endoplasmic reticulum resident heat shock protein gp96 triggers MyD88-dependent systemic autoimmune diseases. *Proc. Natl Acad. Sci. USA* 100(26), 15824–15829 (2003).

49 Dai J, Liu B, Cua DJ, Li Z. Essential roles of IL-12 and dendritic cells but not IL-23 and macrophages in lupus-like diseases initiated by cell surface HSP gp96. *Eur. J. Immunol.* 37(3), 706–715 (2007).

50 Baker-Lepain JC, Sarzotti M, Nicchitta CV. Glucose-regulated protein 94/glycoprotein 96 elicits bystander activation of $CD4^+$ T cell Th1 cytokine production *in vivo*. *J. Immunol.* 172(7), 4195–4203 (2004).

51 Henderson B, Calderwood SK, Coates AR *et al.* Caught with their PAMPs down? The extracellular signalling actions of molecular chaperones are not due to microbial contaminants. *Cell Stress Chaperones* 15(2), 123–141 (2010).

▪▪ **Overview of extracellular HSPs and innate immune responses.**

52 Andersson U, Tracey KJ. HMGB1 is a therapeutic target for sterile inflammation and infection. *Annu. Rev. Immunol.* 29, 139–162 (2011).

53 Yu M, Wang H, Ding A *et al.* HMGB1 signals through toll-like receptor (TLR) 4 and TLR2. *Shock* 26(2), 174–179 (2006).

54 Yamasaki S, Ishikawa E, Sakuma M, Hara H, Ogata K, Saito T. Mincle is an ITAM-coupled activating receptor that senses damaged cells. *Nat. Immunol.* 9(10), 1179–1188 (2008).

55 Moussion C, Ortega N, Girard JP. The IL-1-like cytokine IL-33 is constitutively expressed in the nucleus of endothelial cells and epithelial cells *in vivo*: a novel 'alarmin'? *PLoS ONE* 3(10), E3331 (2008).

56 Cayrol C, Girard JP. The IL-1-like cytokine IL-33 is inactivated after maturation by caspase-1. *Proc. Natl Acad. Sci. USA* 106(22), 9021–9026 (2009).

57 Hofmann MA, Drury S, Fu C *et al.* RAGE mediates a novel proinflammatory axis: a central cell surface receptor for S100/calgranulin polypeptides. *Cell* 97(7), 889–901 (1999).

58 Chen GY, Nunez G. Sterile inflammation: sensing and reacting to damage. *Nat. Rev. Immunol.* 10(12), 826–837 (2010).

59 Tian J, Avalos AM, Mao SY *et al.* Toll-like receptor 9-dependent activation by DNA-containing immune complexes is mediated by HMGB1 and RAGE. *Nat. Immunol.* 8(5), 487–496 (2007).

60 Okuya K, Tamura Y, Saito K *et al.* Spatiotemporal regulation of heat shock protein 90-chaperoned self-DNA and CpG-oligodeoxynucleotide for type I IFN induction via targeting to static early endosome. *J. Immunol.* 184(12), 7092–7099 (2010).

▪ **Demonstrates the spatiotemporal regulation of innate ligand by extracellular Hsp90.**

61 Wagner H. Bacterial CpG DNA activates immune cells to signal infectious danger. *Adv. Immunol.* 73, 329–368 (1999).

62 Krieg A. CpG motifs in bacterial DNA and their immune effects. *Annu. Rev. Immunol.* 20, 709–760 (2002).

63 Lakadamyali M, Rust MJ, Zhuang X. Ligands for clathrin-mediated endocytosis are differentially sorted into distinct populations of early endosomes. *Cell* 124(5), 997–1009 (2006).

64 Yoshida H, Okabe Y, Kawane K, Fukuyama H, Nagata S. Lethal anemia caused by interferon-β produced in mouse embryos carrying undigested DNA. *Nat. Immunol.* 6(1), 49–56 (2005).

65 Minota S, Koyasu S, Yahara I, Winfield J. Autoantibodies to the heat-shock protein Hsp90 in systemic lupus erythematosus. *J. Clin. Invest.* 81(1), 106–109 (1988).

66 Conroy SE, Faulds GB, Williams W, Latchman DS, Isenberg DA. Detection of autoantibodies to the 90 kDa heat shock protein in systemic lupus erythematosus and other autoimmune diseases. *Br. J. Rheumatol.* 33(10), 923–926 (1994).

67 Twomey BM, Dhillon VB, Mccallum S, Isenberg DA, Latchman DS. Elevated levels of the 90 kD heat shock protein in patients with systemic lupus erythematosus are dependent upon enhanced transcription of the Hsp90 β gene. *J. Autoimmun.* 6(4), 495–506 (1993).

68 Ripley BJ, Isenberg DA, Latchman DS. Elevated levels of the 90 kDa heat shock protein (Hsp90) in SLE correlate with levels of IL-6 and autoantibodies to Hsp90. *J. Autoimmun.* 17(4), 341–346 (2001).

69 Perdew GH, Hord N, Hollenback CE, Welsh MJ. Localization and characterization of the 86- and 84-kDa heat shock proteins in Hepa 1c1c7 cells. *Exp. Cell. Res.* 209(2), 350–356 (1993).

70 Akner G, Mossberg K, Sundqvist KG, Gustafsson JA, Wikstrom AC. Evidence for reversible, non-microtubule and non-microfilament-dependent nuclear translocation of Hsp90 after heat shock in human fibroblasts. *Eur. J. Cell. Biol.* 58(2), 356–364 (1992).

71 Lande R, Gregorio J, Facchinetti V *et al.* Plasmacytoid dendritic cells sense self-DNA coupled with antimicrobial peptide. *Nature* 449(7162), 564–569 (2007).

72 Means TK, Latz E, Hayashi F, Murali MR, Golenbock DT, Luster AD. Human lupus autoantibody-DNA complexes activate DCs through cooperation of CD32 and TLR9. *J. Clin. Invest.* 115(2), 407–417 (2005).

73 Shen L, Sigal LJ, Boes M, Rock KL. Important role of cathepsin S in generating peptides for TAP-independent MHC class I crosspresentation *in vivo*. *Immunity* 21(2), 155–165 (2004).

74 Kurotaki T, Tamura Y, Ueda G *et al.* Efficient cross-presentation by heat shock protein 90-peptide complex-loaded dendritic cells via an endosomal pathway. *J. Immunol.* 179(3), 1803–1813 (2007).

75 Oura J, Tamura Y, Kamiguchi K *et al.* Extracellular heat shock protein 90 plays a role in translocating chaperoned antigen from endosome to proteasome for generating antigenic peptide to be cross-presented by dendritic cells. *Int. Immunol.* 23(4), 223–237 (2011).

76 Imai T, Kato Y, Kajiwara C *et al.* Heat shock protein 90 (Hsp90) contributes to cytosolic translocation of extracellular antigen for cross-presentation by dendritic cells. *Proc. Natl Acad. Sci. USA* 108(39), 16363–16368 (2011).

▪ **Demonstrates the impact of endogenous Hsp90 on cross-presentation using Hsp90α-knockout mice.**

77 Murshid A, Gong J, Calderwood SK. Heat shock protein 90 mediates efficient antigen cross presentation through the scavenger receptor expressed by endothelial cells-I. *J. Immunol.* 185(5), 2903–2917 (2010).

78 Burgdorf S, Kautz A, Bohnert V, Knolle PA, Kurts C. Distinct pathways of antigen uptake and intracellular routing in CD4 and CD8 T cell activation. *Science* 316(5824), 612–616 (2007).

79 Burgdorf S, Scholz C, Kautz A, Tampe R, Kurts C. Spatial and mechanistic separation of cross-presentation and endogenous antigen presentation. *Nat. Immunol.* 9(5), 558–566 (2008).

80 Kutomi G, Tamura Y, Okuya K *et al.* Targeting to static endosome is required for efficient cross-presentation of endoplasmic reticulum-resident oxygen-regulated protein 150-peptide complexes. *J. Immunol.* 183(9), 5861–5869 (2009).

81 Borges TJ, Wieten L, Van Herwijnen MJ *et al.* The anti-inflammatory mechanisms of Hsp70. *Front. Immunol.* 3, 95 (2012).

82 Tamura Y, Hirohashi Y, Kutomi G *et al.* Tumor-produced secreted form of binding of immunoglobulin protein elicits antigen-specific tumor immunity. *J. Immunol.* 186(7), 4325–4330 (2011).

83 Facciponte JG, Wang XY, Subjeck JR. Hsp110 and Grp170, members of the Hsp70 superfamily, bind to scavenger receptor-A and scavenger receptor expressed by endothelial cells-I. *Eur. J. Immunol.* 37(8), 2268–2279 (2007).

84 Manjili, MH, Park J, Facciponte JG, Subjeck JR. Hsp110 induces "danger signals" upon interaction with antigen presenting cells and mouse mammary carcinoma. *Immunobiology* 210(5), 295–303 (2005).

85 Park JE, Facciponte J, Chen X *et al.* Chaperoning function of stress protein grp170, a member of the Hsp70 superfamily, is responsible for its immunoadjuvant activity. *Cancer Res.* 66(2), 1161–1168 (2006).

Cell Stress and Chaperones (2012) 17:757–763
DOI 10.1007/s12192-012-0348-0

ORIGINAL PAPER

Heat shock enhances the expression of cytotoxic granule proteins and augments the activities of tumor-associated antigen-specific cytotoxic T lymphocytes

Akari Takahashi · Toshihiko Torigoe · Yasuaki Tamura · Takayuki Kanaseki · Tomohide Tsukahara · Yasushi Sasaki · Hidekazu Kameshima · Tetsuhiro Tsuruma · Koichi Hirata · Takashi Tokino · Yoshihiko Hirohashi · Noriyuki Sato

Received: 1 February 2012 / Revised: 19 June 2012 / Accepted: 21 June 2012 / Published online: 11 July 2012

Abstract Focal inflammation causes systemic fever. Cancer hyperthermia therapy results in shrinkage of tumors by various mechanisms, including induction of adaptive immune response. However, the physiological meaning of systemic fever and mechanisms of tumor shrinkage by hyperthermia have not been completely understood. In this study, we investigated how heat shock influences the adaptive immune system. We established a cytotoxic T lymphocyte (CTL) clone (#IM29) specific for survivin, one of the tumor-associated antigens (TAAs), from survivin peptide-immunized cancer patients' peripheral blood, and the CTL activities were investigated in several temperature conditions (37–41 °C). Cytotoxicity and IFN-γ secretion of CTL were greatest under vh39 °C condition, whereas they were minimum under 41 °C. To address the molecular mechanisms of this phenomenon, we investigated the apoptosis status of CTLs, expression of CD3, CD8, and TCRαβ by flow cytometry, and expression of perforin, granzyme B, and Fas ligand by western blot analysis. The expression of perforin and granzyme B were upregulated under temperature conditions of 39 and 41 °C. On the other hand, CTL cell death was induced under 41 °C condition with highest Caspase-3 activity. Therefore, the greatest cytotoxicity activity at 39 °C might depend on upregulation of cytotoxic granule proteins including perforin and granzyme B. These results suggest that heat shock enhances effector phase of the adaptive immune system and promotes eradication of microbe and tumor cells.

Keywords Heat shock · CTL · Perforin · Survivin

Abbreviations

CTL	Cytotoxic T lymphocyte
TAA	Tumor-associated antigen
HLA	Human leukocyte antigen
PBMC	Peripheral blood mononuclear cell
mAb	Monoclonal antibody
HSP	Heat shock protein

Introduction

Inflammation is defined by four classical signs, pain (dolor), heat (calor), redness (rubor), and swelling (tumor), caused by secretion of inflammatory cytokines (e.g., IL-1β, TNFα, and IL-6) from inflammatory cells (Bernheim et al. 1979). Inflammatory cytokines induce the secretion of prostaglandin E2 from endothelial cells of the central nervous system, and prostaglandin E2 acts in the hypothalamic area, resulting in fever. Although fever is one of the well-described symptoms of

Electronic supplementary material The online version of this article (doi:10.1007/s12192-012-0348-0) contains supplementary material, which is available to authorized users.

A. Takahashi · T. Torigoe (✉) · Y. Tamura · T. Kanaseki · T. Tsukahara · Y. Sasaki · Y. Hirohashi (✉) · N. Sato
Department of Pathology,
Sapporo Medical University School of Medicine,
South-1 West-17, Chuo-Ku,
Sapporo 060-8556, Japan
e-mail: torigoe@sapmed.ac.jp
e-mail: hirohash@sapmed.ac.jp

Y. Sasaki · T. Tokino
Department of Medical Genome Sciences,
Research Institute for Frontier Medicine,
Sapporo Medical University School of Medicine,
South-1 West-17, Chuo-Ku,
Sapporo 060-8556, Japan

H. Kameshima · T. Tsuruma · K. Hirata
Department of Surgery,
Sapporo Medical University School of Medicine,
South-1 West-17, Chuo-Ku,
Sapporo 060-8556, Japan

Table 1 Summary of antibodies

Antigen	Company	Clone	Dilution	Application
CD3	Beckman Coletr	UCHT1		Flow cytometry
CD8	BD	SK1		Flow cytometry
TCRαβ	Thermo scientific	BMA031		Flow cytometry
HLA-A24	–[a]	C7709A2.6	Culture sup.	Flow cytometry
Fas Ligand	MBL	CH-11	1000	Western blot
Perforin	SIGMA	3B4	1000	Western blot
Granzyme B	R&D systems	351927	1000	Western blot
HSP90	Enzo Life Sciences	AC88	1000	Western blot
HSP70	Enzo Life Sciences		1000	Western blot
Fas Ligand	R&D systems	#154922	1000	Western blot
β-actin	SIGMA	AC15	2000	Western blot

[a]Kind gift from Dr. P. G. Coulie

inflammation, the physiological meanings on adaptive immunity involving cytotoxic T lymphocytes (CTLs) still remain unclear.

Hyperthermia for cancer treatment has been of clinical interest for many years, though the exact anti-tumor mechanism remains unclear. Several reports have indicated that heat treatment enhanced adaptive immune response by CTL cross-priming due to induction of heat shock proteins (HSPs). HSPs associated with antigenic peptides and HSPs induced by heat treatment in cancer cells enhance cancer-specific adaptive immune responses by cross-priming (Bachleitner-Hofmann et al. 2006; Brusa et al. 2009; Sato et al. 2009, 2010; Shi et al. 2006; Torigoe et al. 2009). On the other hand, the direct effects of heat treatment on established CTLs remain unknown.

In this study, we investigated the effect of heat treatment on a CTL clone specific for survivin, one of the tumor-associated antigens (TAAs; Hirohashi et al. 2002). Heat treatment (39 °C) of CTLs enhanced the cytotoxicity and the secretion of IFN-γ of CTLs, whereas heat treatment with higher temperature (41 °C) abrogated CTL functions. To address the molecular mechanism of this phenomenon, we examined changes in the expression of several molecules in CTLs and found that the expression of cytotoxic granule proteins (perforin and granzyme B) is enhanced by heat treatment. On the other hand, the expression of CD3, CD8, and TCR B did not show any difference. The viability of CTLs was abrogated and apoptotic cells were increased by higher heat treatment (41 °C). These findings indicate that heat treatment of CTLs at 39 °C enhances CTL functions

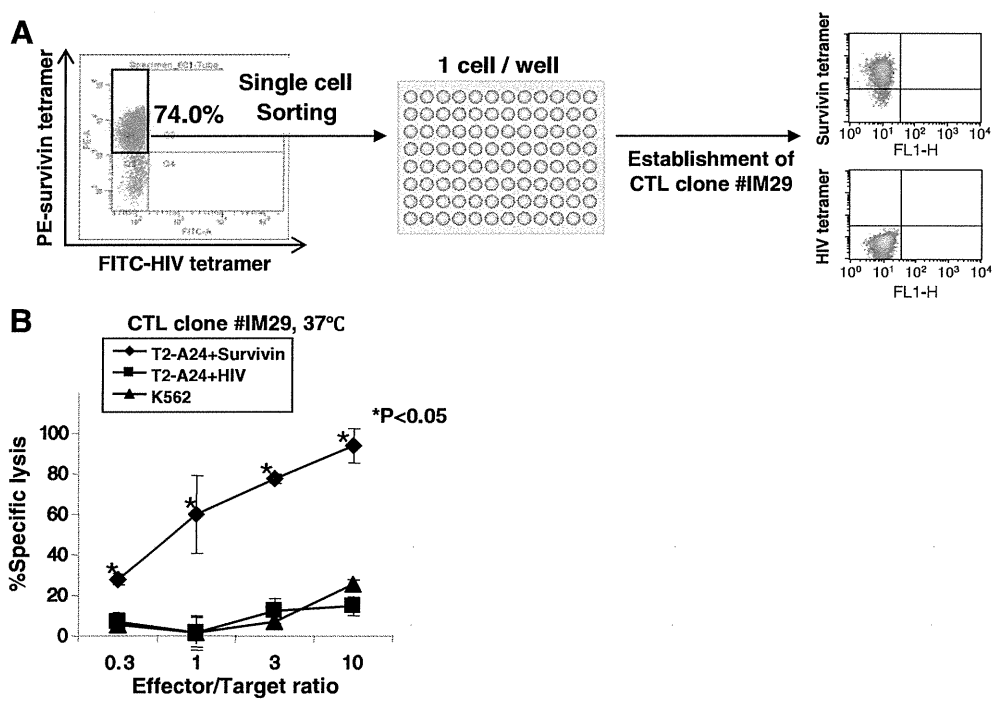

Fig. 1 Establishment of CTL clone #IM29. **a** Schematic summary of establishment of CTL clone. Survivin tetramer-positive cells were single-cell-sorted into a 96-well plate at single cell per well. The specificity of growing T cells was assessed by survivin- and HIV-tetramer staining. **b** Cytotoxicity of CTL clone #IM29. Cytotoxicity of CTL clone #IM29 was evaluated with survivin peptide-pulsed T2-A24 cells, control peptide (HIV)-pulsed T2-A24 cells and K562 cells. *Asterisks* represent significant difference compared with HIV peptide-pulsed T2-A24 cells or K562 cells ($P<0.05$, t test). Data are mean±SD

partially by upregulation of perforin and granzyme B, and that heat treatment of CTLs at 41 °C abrogates CTL functions partially by inducing apoptosis. Augmentation of CTL functions by heat treatment might be one significant reason of fever induced by inflammation and also one mechanism of hyperthermia.

Materials and methods

Cells and antibodies

T2-A24 cells, human leukocyte antigen (HLA)-A24 gene-transduced T2 cells, were a kind gift from Dr. K. Kuzushima (Nagoya, Japan). The cells were cultured in RPMI1640 (SIGMA) supplemented with 10 % FBS (Life Technologies) and 800 μg/ml of G418 (Life Technologies). K562 cells were obtained from ATCC and cultured in RPMI1640 supplemented with 10 % FBS. The antibodies used in this study are summarized in Table 1.

Establishment of CTL clone #IM29

A survivin peptide-specific CTL clone was established from peripheral blood of a 44-year-old patient with rectal carcinoma who was treated with survivin peptide immunization and IFNα (Kameshima et al. 2011). Survivin peptide-specific CTLs were stained with survivin peptide-HLA-A24 complex tetramer and were single-cell-sorted by FACS Aria II (BD) into a round-bottomed 96-well plate at single cell per well. The CTL was incubated with irradiated 8×10^4 peripheral blood mononuclear cells (PBMCs) in AIM-V (Life Technologies) medium supplemented with 10 % human AB serum (kindly provided by Dr. Tatsuo Usui, Hokkaido Red

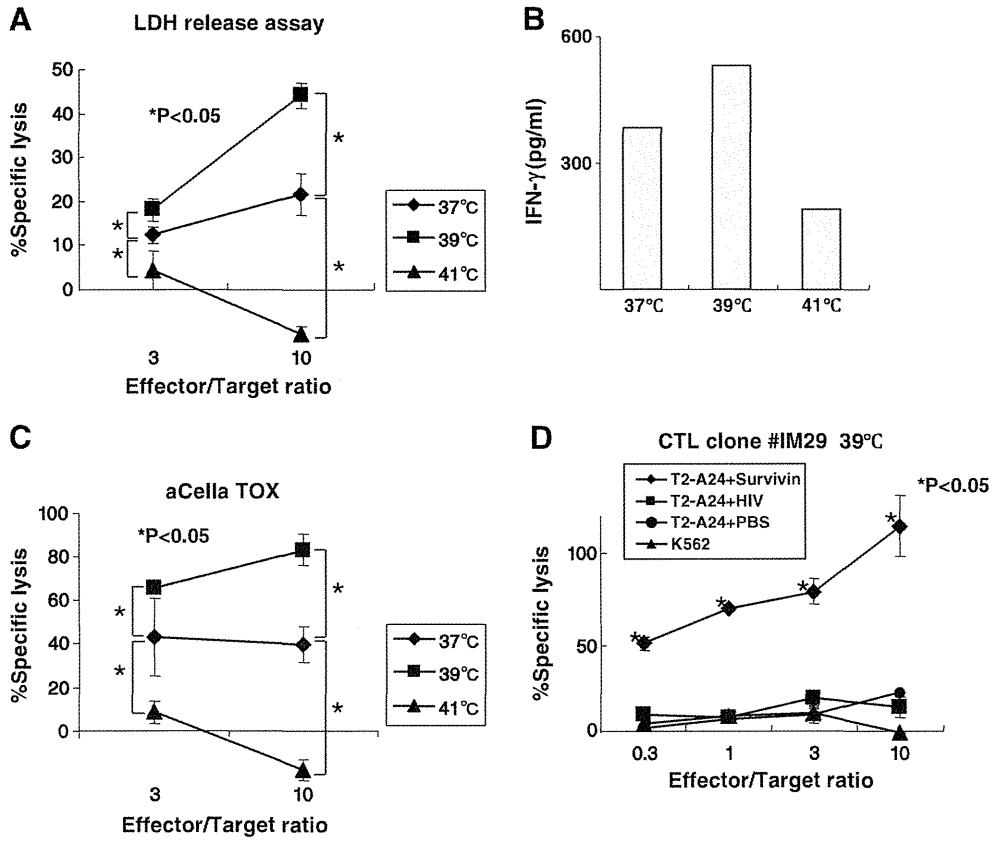

Fig. 2 Heat treatment enhances CTL functions. **a** Cytotoxicity of CTL clone #IM29 in several temperature conditions. Cytotoxicity of CTL clone #IM29 using T2-A24 cells pulsed with survivin peptide was evaluated by LDH release assay under several temperature conditions (37, 39, and 41 °C). *Asterisks* represent significant difference ($P<0.05$, *t* test). Data are mean±SD. **b** IFN-γ secretion of CTL clone #IM29 in several temperature conditions. IFN-γ secretion of CTL clone #IM29 using T2-A24 cells pulsed with survivin peptide was evaluated by ELISA under several temperature conditions (37, 39, and 41 °C). Data are mean. **c** Cytotoxicity of CTL clone #IM29 using aCella TOX assay. Cytotoxicity of CTL clone #IM29 using T2-A24 cells pulsed with survivin peptide was evaluated by aCella TOX assay under several temperature conditions (37, 39, and 41 °C). *Asterisks* represent significant difference ($P<0.05$, *t* test). Data are mean ± SD. **d** Cytotoxicity of CTL clone #IM29 in 39 °C condition. CTLs were preincubated in 39 °C for 1 day before cytotoxicity assay. Cytotoxicity of CTL clone #IM29 was evaluated with survivin peptide-pulsed T2-A24 cells, control peptide (HIV)-pulsed T2-A24 cells and K562 cells in 39 °C. *Asterisks* represent significant difference compared with HIV peptide-pulsed T2-A24 cells or K562 cells ($P<0.05$, *t* test). Data are mean±SD

Cross Blood Center, Sapporo, Japan), 200 IU of IL-2 (R&D Systems), and 5 μg/ml of PHA (SIGMA). Growing wells were transferred into a 24-well plate and fed every 3 days with AIM-V supplemented with 10 % human AB serum and 200 IU of IL-2. On day 34, clones were assessed by survivin tetramer staining and HIV-tetramer as a negative control (Fig. 1a). Tetramers were obtained from MBL Co., Ltd. (Nagoya, Japan).

Cytotoxicity assay and IFN-γ ELISA

CTL clone #IM29 were preincubated at 37–41 °C for 1 day before cytotoxicity assay and IFN-γ ELISA. Survivin peptide-pulsed T2-A24 cells were seeded into a 96-well plate at 5×10^3 cells/well. CTL clone #IM29 cells were seeded at several effector/target (*E/T*) ratios, then incubated at 37–41 °C for 6 h. Cytotoxicity of CTL clone #IM29 cells was examined by using an LDH cytotoxicity detection kit (TAKARA BIO Inc., Osaka, Japan) and aCella TOX kit (Cell Technology, Inc., Mountain View, CA) according to the manufacturer's protocol.

Ten thousand survivin peptide-pulsed T2-A24 cells and 3×10^3 of CTL clone #29 cells were co-cultured in a 96-well plate at 37–41 °C for 12 h, and then IFN-γ concentrations in supernatants were measured by using a Human IFN gamma ELISA Kit (Thermo Scientific) as described in the manufacturer's protocol.

Live images of cytotoxicity were recorded by the OLYMPUS FLUOVIEW FV 300-I71BG-SP system (OLYMPUS). Briefly, T2-A24 cells were transduced with GFP-plasmid using a Nucleofector V kit (Amaxa). GFP-positive T2-A24 cells were pulsed with survivin peptide and co-cultured with CTL clone #IM29 cells at an *E/T* ratio=10, and cultured in 37–41 °C for 4 h and live image were recorded.

Flow cytometry

For detection of HLA-A24 of T2-A24 cells, T2-A24 cells were stained with anti-HLA-A24 mAb (C7709A2.6, kind gift from Dr. P. G. Coulie, Brussels, Belgium) for 1 h, washed three times with PBS, stained with FITC-labeled anti-mouse IgG+M antibody (KPL, 200 times dilution) for 30 min, and washed again one time with PBS. T2-A24 cells were analyzed by a FACS Calibur (BD).

After treatment of CTL clone #IM29 cells at 37–41 °C for 12 h, the expression of CD3, CD8, and TCRαβ was examined by ad FACS Calibur. After staining with first antibodies (summarized in Table 1), CTL clone #IM29 cells were stained with FITC-labeled anti-mouse IgG+M antibody and then analyzed by a FACS Calibur. Mean fluorescent intensity was calculated by CELL Quest software (BD).

Western blot

Western blot analysis was performed as described previously (Nakatsugawa et al. 2011). Anti-perforin, granzyme B, Fas ligand, HSP90, and β-actin mAbs were used at 1,000×, 1,000×, 1,000×, 1,000×, and 2,000× dilutions, respectively (summarized in Table 1). The specific bands were quantified by using Image J software (NIH).

Detection of apoptosis

Apoptotic cells were detected by staining with anti-annexin V antibody and propidium iodide (PI) using annexin V FLUOD staining kit (Roche) according to the manufacturer's protocol and then analyzed by a FACS Calibur. For detection of dead cells, CTLs were stained with Trypan Blue (Life Technologies) and % dead cells were calculated by Countess Automated Cell Counter (Life Technologies). Caspase-3 activity was measured by using APOPCYTO Caspase-3 Colorimetric Assay Kit (MBL, Nagoya, Japan) according to the manufacturer's protocol. CTLs were preincubated under 37–41 °C conditions for 24 h, before caspase-3 assay.

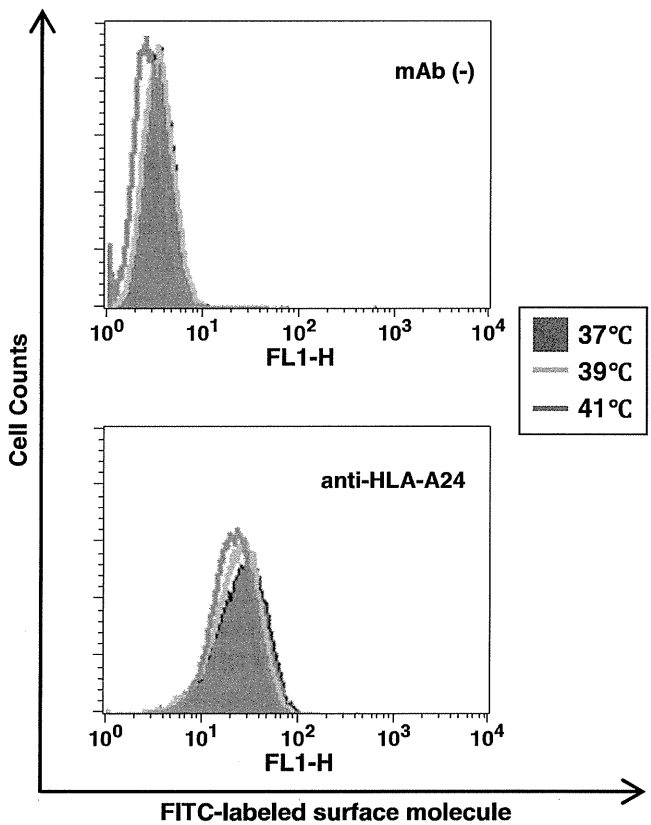

Fig. 3 Heat shock did not alter HLA-A24 expression on T2-A24 cells. The expression of HLA-A24 on T2-A24 cells under several temperature conditions was evaluated by a FACS Calibur. Mean fluorescent intensity (MFI) are listed in ESM 5

Results

Establishment of survivin-derived antigenic peptide-specific CTL clone

To establish a CTL clone specific for cancer cells, we sorted survivin peptide-specific CTLs using survivin peptide-HLA-A24 complex tetramer (Fig. 1a). Sorted CTLs were grown in 96-well plates and a survivin tetramer-positive CTL clone (#IM29) was established (Fig. 1a). CTL clone #IM29 recognized survivin peptide-pulsed T2-A24 cells at different *E/T* ratios, whereas it did not recognize control peptide-pulsed T2-A24 cells or K562 cells, indicating that CTL clone #IM29 is specific for survivin peptide (Fig. 1b).

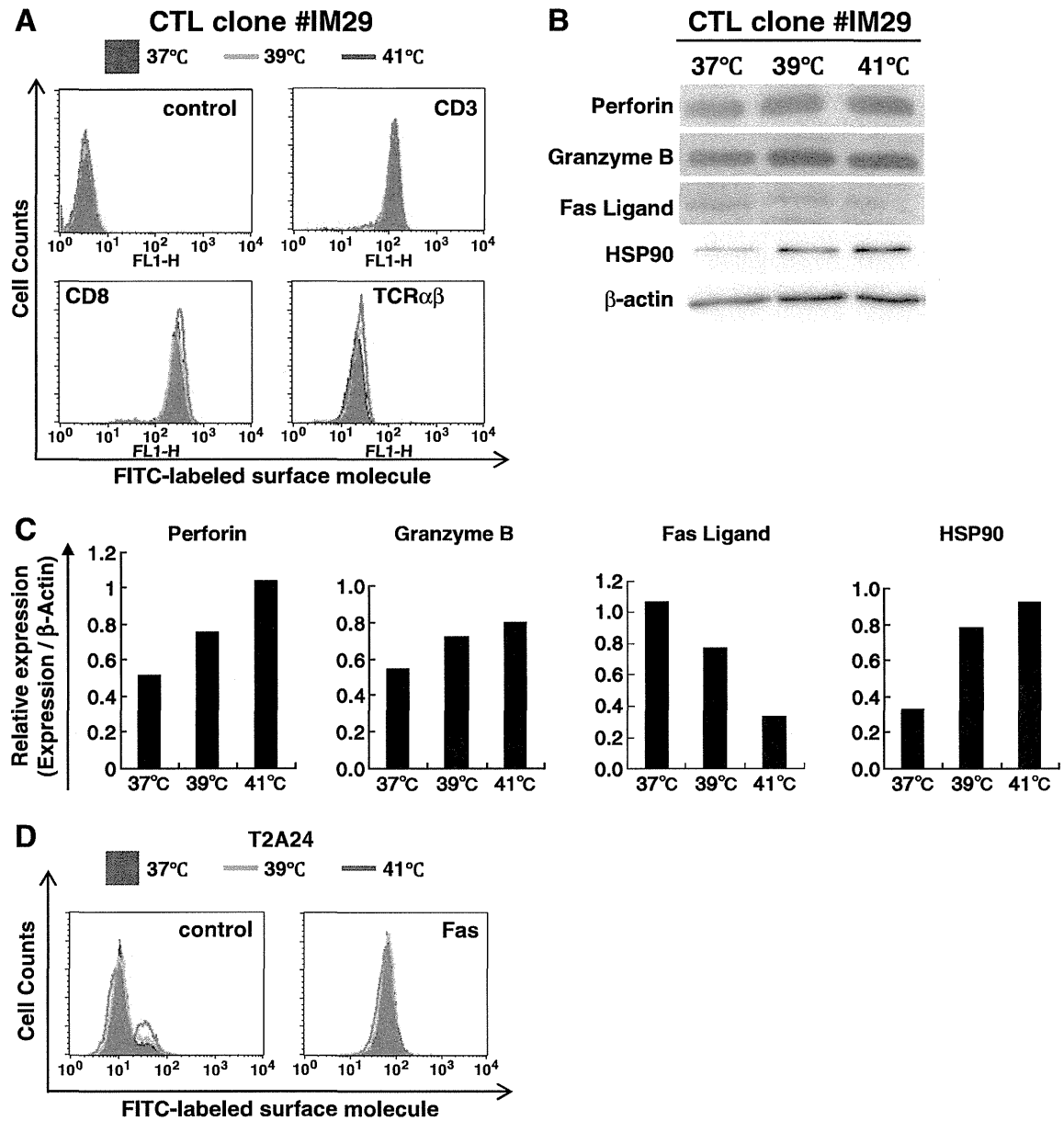

Fig. 4 Expression of several molecules of CTL in several temperature conditions. **a** Flow cytometer analysis of surface molecules on CTL clone #IM29 cells under several temperature conditions. CD3, CD8 and TCRαβ expression on CTL clone #IM29 under several temperature conditions was analyzed by using a flow cytometer. Mean fluorescent intensity (MFI) are listed in ESM 6. **b** Western blot analysis of CTL clone #IM29 under several temperature conditions. Perforin, granzyme B, Fas ligand and HSP90 protein expression in CTL clone #IM29 under several temperature conditions was analyzed by western blot analysis. β-Actin was uses as a internal positive control. Data are representative Western Blot pictures. **c** Quantification of protein expression in CTL clone #IM29 under several temperature conditions. Western blot bands were analyzed, and quantified by Image J software (NIH). Perforin, granzyme B, Fas ligand, and HSP90 expression were standardized by β-Actin. Data are relative expression of perforin, granzyme B, Fas ligand and HSP90. **d** Heat shock did not alter Fas expression on T2-A24 cells. The expression of Fas on T2-A24 cells under several temperature conditions was evaluated by a FACS Calibur. Mean fluorescent intensity (MFI) are listed in ESM 7

Heat treatment enhanced CTL functions

To address the effects of heat treatment on CTL functions, we evaluated CTL functions under several temperature (37–41 °C) conditions (Fig. 2a, b, c and Electronic supplementary material (ESM)). Cytotoxicity of CTL was significantly enhanced in 39 °C condition compared with 37 °C condition, whereas the cytotoxicity was decreased in 41 °C condition by LDH release assay (Fig. 2a). IFN-γ secretion also showed similar pattern as cytotoxicity with highest IFN-γ secretion in 39 °C condition (Fig. 2b). To confirm the cytotoxicity results using LDH release assay, we performed aCella TOX assay. aCella TOX assay also showed that the cytotoxicity of CTL was greatest in 39 °C condition, and minimum in 41 °C (Fig. 2c). The specificity of CTL was not altered in 39 °C condition indicating that heat shock enhances only antigenic peptide-specific cytotoxicity, but not non-specific cytotoxicity (Fig. 2d).

Heat shock induced the HSP70 expression in T2-A24 cells (Supplemental data 4), whereas the expression of HLA-A24 molecule on T2-A24 cells was not enhanced under heat shock conditions (Fig. 3).

Heat treatment upregulated the expression of perforin

CTLs recognize target cells through cell surface molecules, including CD3, CD8, and TCRαβ, and kill target cells by secretion of cytotoxic granule proteins including perforin and granzyme B. We investigated the expression of these molecules in CTLs under several temperature conditions (Fig. 4a and b). The expression of CD3, CD8, and TCRαβ on the surface of CTLs were almost the same in all temperature conditions (37–41 °C; Fig. 4a and b). On the other hand, the expression of perforin and granzyme B were enhanced in high temperature conditions (39 °C and 41 °C) compared with its expression in 37 °C condition (Fig. 4b and c). Fas ligand protein, another cytotoxic molecule expression and Fas expression on T2-A24 cells did not show any increase (Fig. 4b and d).

Heat treatment (41 °C) increased apoptotic cell death of CTLs

Since CTL activity was minimum in the condition of 41 °C, we investigated the cell conditions of CTLs in several

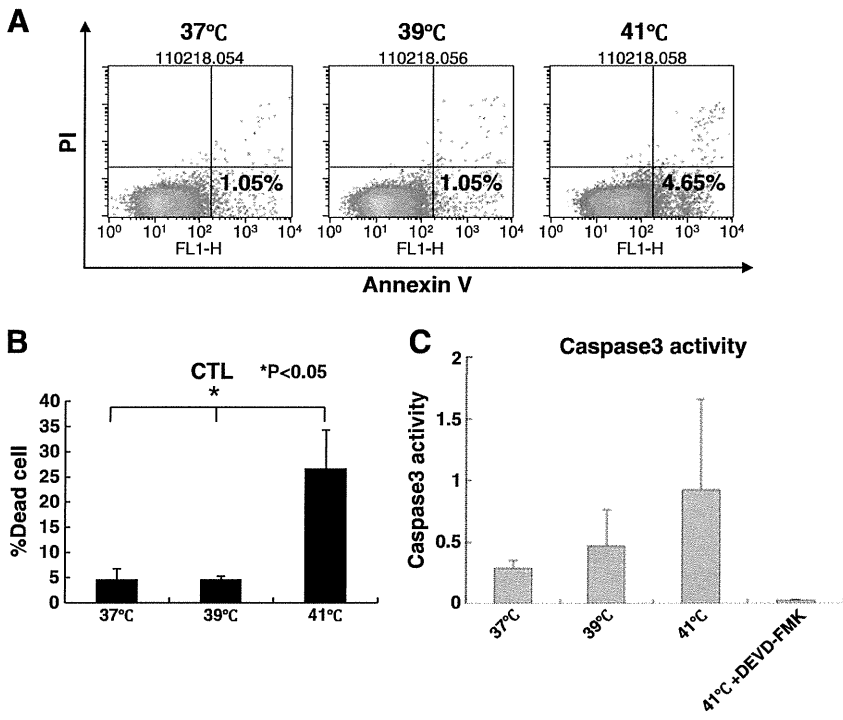

Fig. 5 Apoptotic cell death was induced under 41 °C condition. **a** Detection of apoptosis under several temperature conditions. Apoptotic cell death was detected by anti-annexin V and propidium iodide (PI) staining under several temperature conditions. Percentages represent apoptotic cells (annexin V-positive and PI-negative cells). **b** Percent dead cells was increased in 41 °C. CTLs were preincubated in 37–41 °C for 1 day. CTLs were stained with Trypan Blue and %dead cells were counted by Countess Automated Cell Counter. *Asterisks* represent significant difference ($P<0.05$, *t* test). Data are mean+SD. **c** Caspase 3 was activated in 41 °C. CTLs were preincubated in 37–41 °C for 1 day. Caspase 3 activities were measured by APOPCYTO Caspase-3 Colorimetric Assay Kit. Data are mean+SD

temperature conditions. Trypan Blue staining of CTLs cultured in several temperatures revealed that the percentage of dead cells was highest in 41 °C condition (Fig. 5b). To address the type of cell death, annexin V and PI staining was performed to detect apoptotic cell, which were greater at 41 °C than in other temperature conditions (Fig. 5a); and Caspase-3 activity was highest in the 41 °C condition (Fig. 5c). Thus, the CTL cell death partially by apoptosis under 41 °C condition might be the reason of low CTL activity in high temperature.

Discussion

The physiological meaning of fever caused by inflammation has been a major issue for a long time. In this study, we showed for the first time that CTL activity was upregulated by heat treatment. Results of the cytotoxicity assay and IFN-γ assay showed that CTL activity was greatest at 39 °C and that it was the minimum at 41 °C. These observations indicate that fever caused by systemic inflammatory cytokine release enhances CTL functions, and this might enhance eradication of pathogens. The enhancement of cytotoxicity might depend on upregulation of cytotoxic granule proteins including perforin and granzyme B. After secretion from CTLs, perforin is inserted into the plasma membrane, make pore and lyse target cells. Upregulation of cytotoxic granule proteins might not be involved in the enhancement of IFN-γ secretion, suggesting the existence of another molecular mechanism to enhance CTL functions by heat shock.

The exact molecular mechanisms by which cytotoxic granule proteins are upregulated in heat-treated CTLs remain unclear. Since we treated CTLs at 39 °C, it may be transcription enhanced due to the activation of heat shock factor-1 (HSF1); however, there is no HSF1-binding site (heat shock element) in the promoter region of perforin and granzyme B. (Pipkin et al. 2010) Another possible explanation is stabilization of perforin protein by heat treatment. Heat treatment induces upregulation of several chaperone proteins including HSPs by HSF1, and thus association with these chaperone proteins may stabilize and prolong the life span of cytotoxic granule proteins. Further analysis is needed to clarify the exact molecular mechanisms.

Hyperthermia is one treatment modality for cancers, but the exact mechanisms by which it works to suppress cancers remain unclear. Adaptive immune systems induced by antigenic peptides bound to HSPs might be mechanisms (enhancement of induction phase of CTL). In this study, we showed that heat treatment enhanced the cytotoxicity activity of CTLs (enhancement of effector phase of CTL). Therefore, heat treatment will enhance both induction and effector phases of adaptive immune system. These two mechanisms should act synergistically, and the adaptive immune system should have a role in hyperthermia.

In summary, we showed for the first time that heat treatment of CTLs enhanced CTL functions. Upregulation of cytotoxic granule proteins may play a role in this phenomenon. Enhancement of CTL functions by heat treatment might have a role in CTL functions in fever and hyperthermia.

Acknowledgments The authors thank Ms. E. Nakazawa for technical assistance. The authors thank Dr. Tatsuo Usui (Hokkaido Red Cross Blood Center, Sapporo, Japan) for the kind donation of human sera. The authors thank Dr. K. Kuzushima and Dr. P. G. Coulie for providing cells. This work was supported by Grants-in-Aid for Scientific Research from the Ministry of Education, Culture, Sports, Science and Technology of Japan (grant Nos. 16209013, 17016061 and 15659097) for Practical Application Research from the Japan Science and Technology Agency, and for Cancer Research (15-17 and 19-14) from the Ministry of Health, Labor and Welfare of Japan, Ono Cancer Research Fund (to N. S.) and Takeda Science Foundation (to Y. H.). This work was supported in part by the National Cancer Center Research and Development Fund (23-A-44).

Declaration of financial disclosure The authors have no financial conflict of interest.

References

Bachleitner-Hofmann T et al (2006) Heat shock treatment of tumor lysate-pulsed dendritic cells enhances their capacity to elicit antitumor T cell responses against medullary thyroid carcinoma. J Clin Endocrinol Metab 91:4571–4577

Bernheim HA et al (1979) Fever: pathogenesis, pathophysiology, and purpose. Ann Intern Med 91:261–270

Brusa D et al (2009) Immunogenicity of 56 degrees C and UVC-treated prostate cancer is associated with release of HSP70 and HMGB1 from necrotic cells. Prostate 69:1343–1352

Hirohashi Y et al (2002) An HLA-A24-restricted cytotoxic T lymphocyte epitope of a tumor-associated protein, survivin. Clin Cancer Res 8:1731–1739

Kameshima H et al (2011) Immunogenic enhancement and clinical effect by type-I interferon of anti-apoptotic protein, survivin-derived peptide vaccine, in advanced colorectal cancer patients. Cancer Sci 102:1181–1187

Nakatsugawa M et al (2011) SOX2 is overexpressed in stem-like cells of human lung adenocarcinoma and augments the tumorigenicity. Lab Invest 91:1796–1804

Pipkin ME et al (2010) The transcriptional control of the perforin locus. Immunol Rev 235:55–72

Sato N et al (2009) Molecular pathological approaches to human tumor immunology. Pathol Int 59:205–217

Sato A et al (2010) Melanoma-targeted chemo-thermo-immuno (CTI)-therapy using *N*-propionyl-4-*S*-cysteaminylphenol-magnetite nanoparticles elicits CTL response via heat shock protein–peptide complex release. Cancer Sci 101:1939–1946

Shi H et al (2006) Hyperthermia enhances CTL cross-priming. J Immunol 176:2134–2141

Torigoe T et al (2009) Heat shock proteins and immunity: application of hyperthermia for immunomodulation. Int J Hyperthermia 25:610–616

Tumor Biol. (2012) 33:1307–1317
DOI 10.1007/s13277-012-0378-3

RESEARCH ARTICLE

Genome-wide analysis of DNA methylation identifies novel cancer-related genes in hepatocellular carcinoma

Masahiro Shitani · Shigeru Sasaki · Noriyuki Akutsu · Hideyasu Takagi · Hiromu Suzuki · Masanori Nojima · Hiroyuki Yamamoto · Takashi Tokino · Koichi Hirata · Kohzoh Imai · Minoru Toyota · Yasuhisa Shinomura

Received: 24 January 2012 / Accepted: 11 March 2012 / Published online: 29 March 2012

Abstract Aberrant DNA methylation has been implicated in the development of hepatocellular carcinoma (HCC). Our aim was to clarify its molecular mechanism and to identify useful biomarkers by screening for DNA methylation in HCC. Methylated CpG island amplification coupled with CpG island microarray (MCAM) analysis was carried out to screen for methylated genes in primary HCC specimens [hepatitis B virus (HBV)-positive, n=4; hepatitis C virus (HCV)-positive, n=5; HBV/HCV-negative, n=7]. Bisulfite pyrosequencing was used to analyze the methylation of selected genes and long interspersed nuclear element (LINE)-1 in HCC tissue (n=57) and noncancerous liver tissue (n=50) from HCC patients and in HCC cell lines (n=10). MCAM analysis identified 332, 342, and 259 genes that were methylated in HBV-positive, HCV-positive, and HBV/HCV-negative HCC tissues, respectively. Among these genes, methylation of *KLHL35*, *PAX5*, *PENK*, and *SPDYA* was significantly higher in HCC tissue than in noncancerous liver tissue, irrespective of the hepatitis virus status. LINE-1 hypomethylation was also prevalent in HCC and correlated positively with *KLHL35* and *SPDYA* methylation. Receiver operating characteristic curve analysis revealed that methylation of the four genes and LINE-1 strongly discriminated between HCC tissue and noncancerous liver tissue. Our data suggest that aberrant hyper- and hypomethylation may contribute to a common pathogenesis mechanism in HCC. Hypermethylation of *KLHL35*, *PAX*, *PENK*, and *SDPYA* and hypomethylation of LINE-1 could be useful biomarkers for the detection of HCC.

Keywords Hepatocellular carcinoma · DNA methylation · CpG island · LINE-1 · Biomarker

Electronic supplementary material The online version of this article (doi:10.1007/s13277-012-0378-3) contains supplementary material, which is available to authorized users.

M. Shitani · S. Sasaki (✉) · N. Akutsu · H. Takagi · H. Suzuki · H. Yamamoto · Y. Shinomura (✉)
First Department of Internal Medicine,
Sapporo Medical University,
S1, W16, Chuo-Ku,
Sapporo 060-8543, Japan
e-mail: ssasaki@sapmed.ac.jp
e-mail: shinomura@sapmed.ac.jp

H. Suzuki · M. Toyota
Department of Molecular Biology, Sapporo Medical University,
Sapporo, Japan

M. Nojima
Department of Public Health, Sapporo Medical University,
Sapporo, Japan

T. Tokino
Medical Genome Science, Research Institute for Frontier Medicine, Sapporo Medical University School of Medicine,
Sapporo, Japan

K. Hirata
First Department of Surgery, Sapporo Medical University,
Sapporo, Japan

K. Imai
Division of Novel Therapy for Cancer, The Advanced Clinical Research Center, The Institute of Medical Science,
The University of Tokyo,
Tokyo, Japan

Introduction

Hepatocellular carcinoma (HCC) is one of the most common human malignancies, worldwide [1]. Chronic infection by hepatitis B virus (HBV) and hepatitis C virus (HCV) are well-documented risk factors for the development of HCC, while chronic alcoholism and various environmental factors, including aflatoxin B1, are also believed to be important risk

factors [2, 3]. The development and progression of HCC is often a complex, multistep process entailing the evolution of normal liver through chronic hepatitis and cirrhosis to HCC, but HCC can also arise in a noncirrhotic liver. In either case, the process is influenced by multiple genetic changes, including allelic deletions, chromosomal losses and gains, DNA rearrangements, and gene mutations [4]. In addition, a growing body of evidence suggests that epigenetic changes such as DNA methylation and histone modification also play crucial roles in hepatocarcinogenesis.

Two seemingly contradictory epigenetic events coexist in cancer: global hypomethylation, which is mainly observed in repetitive sequences throughout the genome, and regional hypermethylation, which is frequently associated with CpG islands within gene promoters [5]. Hypermethylation of CpG islands is a common feature of cancer and is associated with gene silencing. Although the classical two-hit theory posits that tumor suppressor genes are inactivated by gene mutation or deletion, it is now recognized that DNA hypermethylation is a third mechanism by which inactivation of tumor suppressor genes occurs, and that it plays a significant role in tumorigenesis. In contrast to the CpG islands, repetitive DNA elements are normally heavily methylated in somatic tissues. About 45 % of the human genome is composed of repetitive sequences, including long interspersed nuclear elements (LINEs) and short interspersed nuclear element [6], and studies have shown that methylation of such repetitive elements can serve as a surrogate for the global methylcytosine content [7]. In that regard, LINE-1 hypomethylation is known to occur during the development of various human malignancies, including HCC [8, 9].

HCC is generally diagnosed at an advanced stage of tumor progression, and a large fraction of HCC cases are fatal. Thus, a better understanding of the underlying molecular mechanisms and identification of genes critical for early detection of HCC and therapeutic intervention would be highly desirable. Although a number of hyper- or hypomethylated loci have been identified in HCC [10–12], only a few studies have been conducted to unravel the genome-wide methylation status [13–15]. In the present study, we carried out genome-wide CpG island methylation analysis in a set of primary HCC specimens, with and without hepatitis virus infection. We also evaluated the hypomethylation of LINE-1 and assessed its association with aberrant CpG island hypermethylation in HCC.

Materials and methods

Tissue samples and cell lines

A total of 57 primary HCC specimens (HBV-positive, n=21; HCV-positive, n=21; HBV/HCV-negative, n=15) were obtained through surgical resection or needle biopsy at Sapporo Medical University Hospital. Corresponding samples of noncancerous liver tissue were also obtained from 50 patients. HBV surface (HBs) antigen and anti-HCV antibody were measured serologically. An informed consent was obtained from all patients before collection of the specimens. The ten liver cancer cell lines (HT17, PLC/PRF/5, Li-7, huH-1, HuH-7, HepG2, Hep3B, HLE, HLF, and JHH-4) used have been described previously [11]. To analyze restoration of gene expression, cells were treated with 2.0 μM 5-aza-2′-deoxycytidine (5-aza-dC) (Sigma, St Louis, MO, USA) for 72 h, replacing the drug and medium every 24 h. Genomic DNA was extracted using the standard phenol–chloroform procedure. Total RNA was extracted using TRIZOL reagent (Invitrogen, Carlsbad, CA, USA) and then treated with a DNA-free kit (Ambion, Austin, TX, USA). Genomic DNA and total RNA from normal liver tissue from a healthy individual were purchased from BioChain (Hayward, CA, USA).

Methylated CpG island amplification coupled with CpG island microarray

Methylated CpG island amplification (MCA) was performed as described previously [13]. Briefly, 500 ng of genomic DNA was digested with the methylation-sensitive restriction endonuclease *Sma*I (New England Biolabs, Ipswich, MA, USA), after which it was digested with the methylation-insensitive restriction endonuclease *Xma*I. The adaptors were prepared by addition of the oligonucleotides RMCA12 (5′-CCGGGCAGAAAG-3′) and RMCA24 (5′-CCACCGCCATCCGAGCCTTTCTGC-3′). After ligation of the digested DNA to the adaptors, PCR amplification was carried out. Using a BioPrime Plus Array CGH Genomic Labeling System (Invitrogen), MCA amplicons from the HCC samples were labeled with Alexa Fluor 647, while amplicons from a normal liver sample was labeled with Alexa Fluor 555. The labeled MCA amplicons were then hybridized to a custom human CpG island microarray containing 15,134 probes covering 6,157 unique genes (G4497A; Agilent Technologies, Santa Clara, CA, USA) [16]. After washing, the array was scanned using an Agilent DNA Microarray Scanner (Agilent technologies), and the data were processed using Feature Extraction software ver. 10.7 (Agilent Technologies). The data were then analyzed using GeneSpring GX ver. 11 (Agilent Technologies).

Methylation-specific PCR

Genomic DNA (1 μg) was modified with sodium bisulfite using an EpiTect Bisulfite Kit (Qiagen, Hilden, Germany), and methylation-specific PCR (MSP) was performed as described previously [17]. Briefly, PCR was run in a 25-μl

volume containing 50 ng of bisulfite-treated DNA, 1× MSP buffer [67 mM Tris–HCl (pH 8.8), 16.6 mM $(NH4)_2SO_4$, 6.7 mM $MgCl_2$, and 10 mM 2-mercaptoethanol], 1.25 mM dNTP, 0.4 μM each primer, and 0.5 U of JumpStart REDTaq DNA Polymerase (Sigma). The PCR protocol for MSP entailed 5 min at 95°C; 35 cycles of 30 s at 95°C, 30 s at 60°C, and 30 s at 72°C; and a 7 min final extension at 72°C. Primer sequences and PCR product sizes are shown in Supplementary Table 1.

Bisulfite pyrosequencing analysis

Bisulfite pyrosequencing analysis was performed as described previously [17]. The PCR protocol entailed 5 min at 95°C; 45 cycles of 1 min at 95°C, 1 min at 60°C, and 1 min at 72°C; and a 7-min final extension at 72°C. PCR products were then bound to Streptavidin Sepharose beads HP (Amersham Biosciences, Piscataway, NJ); after which, the beads containing the immobilized PCR product were purified, washed, and denatured using a 0.2 M NaOH solution. After addition of 0.3 μM sequencing primer to the purified PCR product, pyrosequencing was carried out using a PSQ96MA system (Qiagen, Hilden, Germany) and Pyro Q-CpG software (Qiagen). Primer sequences and PCR product sizes are shown in Supplementary Table 1.

Quantitative RT-PCR

Single-stranded cDNA was prepared using SuperScript III reverse transcriptase (Invitrogen). Quantitative RT-PCR was carried out using TaqMan Gene Expression Assays (*KLHL35*, Hs00400533_m1; *PAX5*, Hs00172003_m1; *PENK*, Hs00175049_m1; *SPDYA*, Hs00736925_m1; *GAPDH*, Hs99999905_m1; Applied Biosystems, Foster City, CA, USA) and a 7500 Fast Real-Time PCR System (Applied Biosystems) according to the manufacturer's instructions. SDS1.4 software (Applied Biosystems) was used for comparative delta Ct analysis, and *GAPDH* served as an endogenous control.

Statistical analysis

To compare differences in continuous variables between groups, *t* tests or ANOVA with post hoc Tukey's tests were performed. Fisher's exact test or chi-squared test was used for analysis of categorical data. Receiver operator characteristic (ROC) curves were constructed based on the levels of methylation. Values of $P<0.05$ (two-sided) were considered statistically significant. Statistical analyses were carried out using SPSS statistics 18 (IBM Corporation, Somers, NY, USA) and GraphPad Prism ver. 5.0.2 (GraphPad Software, La Jolla, CA, USA).

Results

Genome-wide CpG island methylation analysis in HCC

To screen for CpG island hypermethylation in HCC, we carried out methylated CpG island amplification coupled with CpG island microarray (MCAM) analysis using a set of HCC tissue specimens (HBV-positive, $n=4$; HCV-positive, $n=5$; HBV/HCV-negative, $n=7$). As in an earlier study in which the same array system was used, we utilized a signal ratio (Cy5/Cy3) of >2.0 as the criterion for a methylation-positive probe [13]. The average number of methylated probe sets in the HCC specimens was 566 (range 159–846). To assess the association between hepatitis virus infection and methylation status, we categorized the HCC specimens according to their viral status. The average numbers of methylated probe sets in HBV-positive, HCV-positive, and the HBV/HCV-negative HCC specimens were 574, 598, and 539, respectively, which did not significantly differ ($P=0.840$). Interestingly, however, the numbers of methylated probe sets were more varied among HBV/HCV-negative HCCs, which is indicative of their varied pathological backgrounds (Fig. 1a).

To identify commonly methylated genes in HCC, we selected genes that were methylated in at least two tumors in each group. Among the HBV-positive HCCs, 443 probe sets (corresponding to 332 unique genes) satisfied this criterion. Among the HCV-positive HCCs, 476 probe sets (342 unique genes) satisfied the criterion, and among the HBV/HCV-negative HCCs, 348 probe sets (259 unique genes) satisfied the criterion. Collectively, 714 probes (514 unique genes) were selected as commonly methylated genes. Of those, 137, 146, and 47 probe sets were methylated in only HBV-positive, HCV-positive, or HBV/HCV-negative HCC tissues, respectively (Fig. 1b). By contrast, a large number of genes were methylated in multiple categories, and 169 probe sets were methylated in all three groups (Fig. 1b). Consistent with the above results, unsupervised hierarchical clustering analysis demonstrated that some genes were methylated irrespective of the hepatitis virus status, and that HCV-positive HCCs exhibited the largest number of methylated genes (Fig. 1c, Supplementary Fig. 1). Gene ontology analysis of the commonly methylated genes revealed that genes related to "multicellular organismal process," "developmental process," and "system development" are significantly enriched among the methylated genes (Supplementary Table 2). In addition, pathway analysis suggested that some of the methylated genes are involved in differentiation and development (Supplementary Fig. 2).

Identification of novel genes methylated in HCC

Our MCAM analysis suggested that some genes were methylated in a hepatitis virus-specific manner, but a larger

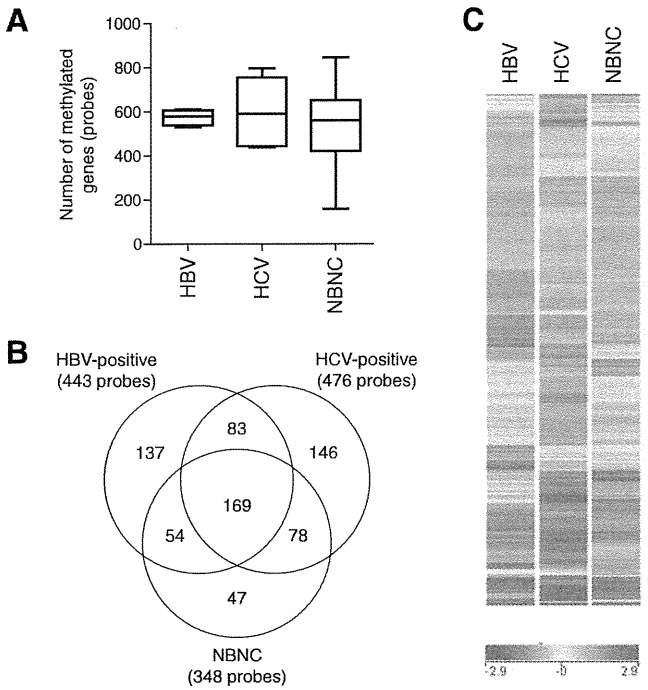

Fig. 1 Genome-wide analysis of CpG island methylation. **a** MCAM analysis was carried out using a series of HCC tissue specimens (HBV-positive, $n=4$; HCV-positive, $n=5$; HBV/HCV-negative, NBNC, $n=7$). MCAM data were categorized into three groups based on the hepatitis virus status, and the numbers of methylated genes in the respective categories are shown. **b** Venn diagram analysis of the methylated genes in the indicated categories. **c** Gene tree view of the MCAM analysis results. A set of 714 probes (514 unique genes) were selected as commonly methylated genes, after which, hierarchical clustering was performed. Each row represents a single probe

number were commonly methylated in HCC. Because recent studies have suggested that aberrant DNA methylation could be a useful diagnostic marker for HCC, we next aimed to identify novel genes frequently methylated in HCC. Among the genes commonly methylated irrespective of hepatitis virus status, we selected 14 (*KLHL35*, *PAX5*, *PENK*, *SPDYA*, *LTBP2*, *DLX1*, *PGBD1*, *WNT9A*, *ADRA1A*, *RHOBTB1*, *GDNF*, *WNT11*, *MLL*, and *PLEC1*) and carried out MSP to assess their methylation status in a series of HCC cell lines (Supplementary Fig. 3). We found that four (*KLHL35*, *PAX5*, *PENK*, and *SPDYA*) of the genes were frequently methylated in HCC cell lines, but showed only little or no methylation in normal liver tissue from a healthy individual (Supplementary Fig. 3). We therefore used quantitative bisulfite pyrosequencing to further analyze the methylation levels of these four genes (Supplementary Figs. 4 and 5).

To determine the extent to which these genes are aberrantly methylated in primary tumors, we analyzed a set of primary HCC specimens (HBV-positive, $n=21$; HCV-positive, $n=21$; HBV/HCV-negative, $n=15$) and corresponding noncancerous liver tissues from the same patients (HBV-positive, $n=18$; HCV-positive, $n=18$; HBV/HCV-negative, $n=14$). Bisulfite pyrosequencing analysis revealed the methylation levels of the four genes to be significantly higher in tumor tissues than in their noncancerous counterparts (*KLHL35*, 37.9 vs. 10.4 %, $P<0.001$; *PAX5*, 23.4 vs. 7.7 %, $P<0.001$; *PENK* 41.1 vs. 22.0 %, $P<0.001$; *SPDYA*, 49.7 vs. 19.3 %, $P<0.001$) (Supplementary Fig. 6). Moreover, these genes were frequently methylated in HCCs, irrespective of the hepatitis virus infection (*KLHL35*, HBV-positive, 37.5 vs. 9.9 %, $P<0.001$; HCV-positive, 38.3 vs. 9.0 %, $P<0.001$; HBV/HCV-negative, 37.7 vs. 13.0 %, $P<0.001$; *PAX5*, HBV-positive, 22.2 vs. 7.6 %, $P=0.014$; HCV-positive, 26.5 vs. 7.2 %, $P<0.001$; HBV/HCV-negative, 20.7 vs. 8.5 %, $P=0.017$; *PENK*, HBV-positive, 45.1 vs. 20.9 %, $P<0.001$; HCV-positive, 39.2 vs. 23.5 %, $P=0.001$; HBV/HCV-negative, 38.2 vs. 21.3 %, $P=0.006$; *SPDYA*, HBV-positive, 51.5 vs. 19.8 %, $P<0.001$; HCV-positive, 46.6 vs. 15.3 %, $P<0.001$; HBV/HCV-negative, 51.3 vs. 23.7 %, $P<0.001$) (Fig. 2a). The association between the methylation of each gene and the clinicopathological features are shown in Table 1. Methylation of *KLHL35* and *PAX5* was correlated with greater age, and *SPDYA* methylation was moderately correlated with higher PIVKA-II levels, but we found no other significant correlations (Table 1). We also generated an ROC curve and observed that methylation of the four genes discriminated strongly between tumor tissues and noncancerous liver tissue, suggesting that methylation of these genes could be a useful tumor marker (Fig. 2b). The most discriminating cutoffs for *KLHL35*, *PAX5*, *PENK*, and *SPDYA* were 14.8 % (sensitivity, 82.5 %; specificity, 88.0 %), 12.5 % (sensitivity, 63.2 %; specificity, 94.0 %), 28.4 % (sensitivity, 70.2 %; specificity, 96.0 %), and 30.3 % (sensitivity, 86.0 %; specificity, 94.0 %), respectively.

Analysis of *KLHL35*, *PAX5*, *PENK*, and *SPYDA* methylation and expression

We next tested whether methylation of *KLHL35*, *PAX5*, *PENK*, and *SPYDA* was associated with their silencing in HCC. Bisulfite pyrosequencing analysis revealed that the degree to which these genes were methylated varied among the HCC cell lines, but it was always much higher than in normal liver tissue from a healthy individual (Fig. 3a). Quantitative RT-PCR analysis confirmed an inverse relationship between methylation and expression of *KLHL35*

Fig. 2 Quantitative methylation analysis of the genes identified by MCAM. **a** Summary of the bisulfite pyrosequencing analysis of *KLHL35*, *PAX5*, *PENK*, and *SPDYA* in tumor tissue (*T*) and noncancerous liver tissue (*N*) from HBV-positive, HCV-positive, and HBV/HCB-negative (NBNC) HCC patients. **b** ROC curve analysis of the methylation of the indicated genes. The area under the ROC curve (*AUC*) for each site conveys its utility (in terms of sensitivity and specificity) for distinguishing between HCC tissue and corresponding noncancerous liver tissue from the same HCC patients

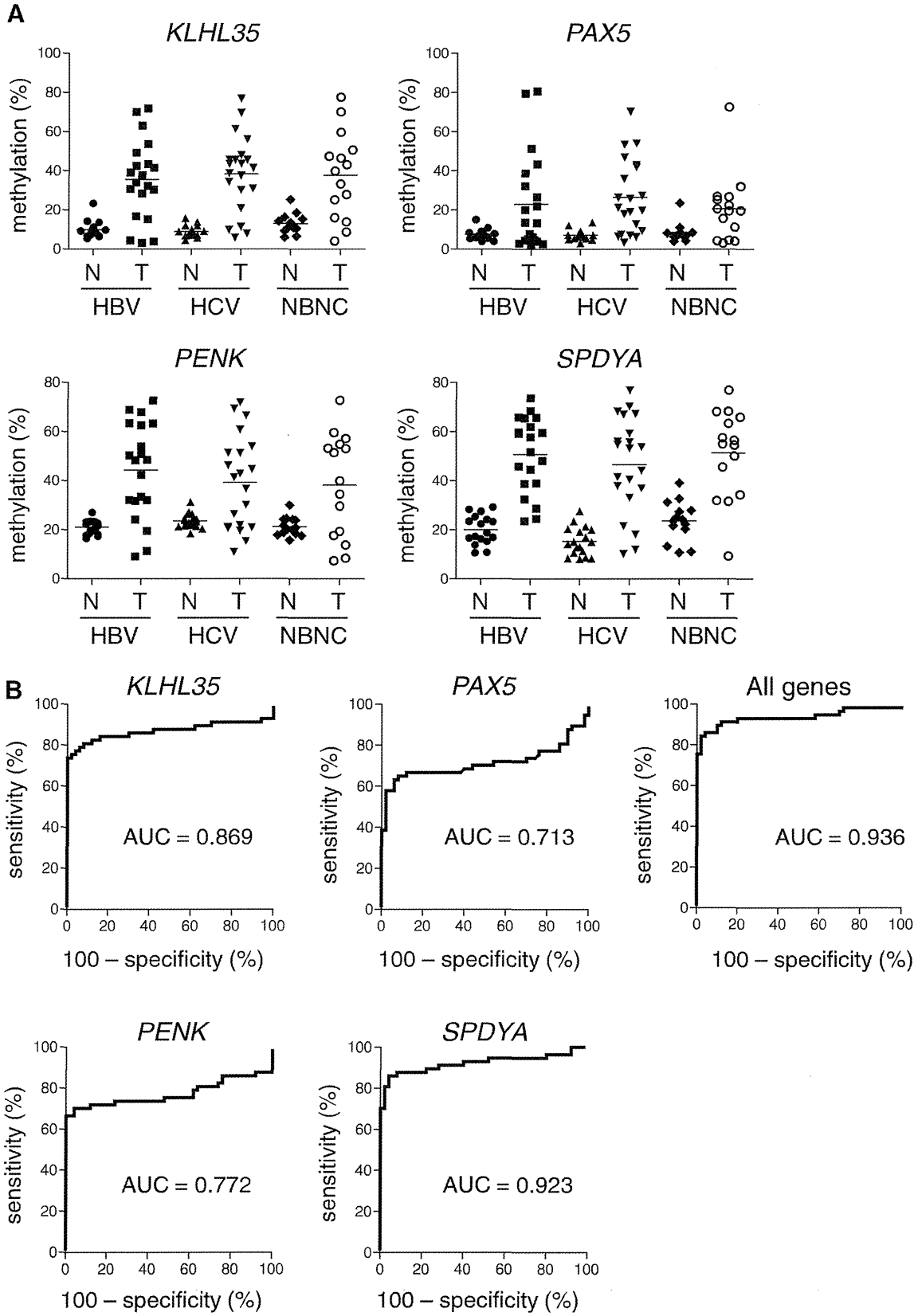

and *PAX5* in the cell lines and normal liver tissue (Fig. 3b), whereas methylation of *PENK* and *SPDYA* did not correlate significantly with their expression levels. The expression of *PENK* was undetectable in seven HCC cell lines and in

Table 1 Association between clinicopathological features and DNA methylation in HCC

	N	*KLHL35* methylation			*PAX5* methylation			*PENK* methylation			*SPDYA* methylation			LINE-1 methylation		
		Mean	SD	*P* value	Mean	SD	*P* value	Mean	SD	*P* value	Mean	SD	*P* value	Mean	SD	*P* value
Age																
≤63	24	30.3	17.7	0.003	18.3	17.1	0.026	41.7	19.3	0.583	51.2	17.9	0.945	49.4	14.8	0.571
>64	23	47.2	18.5		32.3	24.1		44.8	19.6		50.9	15.0		47.2	10.6	
Sex																
M	39	37.5	20.3		22.6	20.9		40.2	19.6		50.1	18.1		47.8	13.3	
F	18	37.2	22.0	0.953	25.2	19.9	0.652	43.1	19.6	0.602	48.7	16.7	0.771	51.5	12.0	0.318
Virus																
HBV	21	35.6	20.3		23.1	24.5		44.3	19.4		50.7	15.4		50.4	13.9	
HCV	21	38.3	19.5		26.5	19.0		39.2	18.8		46.6	19.6		50.2	12.2	
NBNC	15	36.1	22.2	0.900	20.7	17.2	0.698	38.2	21.0	0.603	51.3	18.0	0.668	44.7	12.9	0.359
Child-Pugh																
A	44	39.2	20.0		25.5	22.3		43.4	19.6		51.4	15.6		48.6	12.4	
B	3	29.7	18.2	0.426	19.9	11.8	0.672	41.0	17.1	0.842	45.3	29.5	0.536	44.6	20.6	0.609
PIVKA-II (mAU/ml)																
≤21	16	40.0	19.5		24.0	25.7		42.1	19.1		53.5	14.1		48.0	11.5	
22–66	16	35.8	11.8		23.4	14.2		44.6	14.0		42.9	15.9		52.9	10.7	
>67	15	40.1	26.9	0.795	28.3	24.8	0.802	42.8	24.9	0.933	57.1	16.6	0.039	43.8	15.1	0.136
AFP (ng/ml)																
≤7.4	16	39.3	19.3		25.8	24.1		41.4	19.0		49.4	17.0		47.4	9.2	
7.5–55.0	16	44.9	20.2		31.1	23.2		51.5	15.6		55.0	16.7		50.6	13.4	
>55.1	15	31.1	18.7	0.150	18.1	16.3	0.256	36.3	21.0	0.078	48.7	15.8	0.509	46.9	15.7	0.695
Cirrhosis																
0	27	35.3	23.4		22.2	22.2		40.0	22.1		51.8	18.2		47.7	14.7	
1	24	40.7	16.5	0.353	25.7	20.3	0.559	44.2	17.8	0.467	50.5	15.8	0.795	49.2	11.3	0.687
Vascular invasion																
0	42	38.3	18.5		24.0	21.0		43.9	19.5		52.3	15.1		48.2	12.8	
1	9	35.7	28.9	0.353	23.1	23.3	0.559	33.1	21.5	0.467	46.1	24.2	0.795	49.3	15.1	0.687
TNM stage																
1	6	29.5	15.4		15.0	9.8		50.6	12.1		43.3	20.8		58.4	11.8	
2	20	37.7	20.4		24.6	20.3		44.7	19.3		53.7	11.8		47.5	13.2	
3	13	45.4	14.3		24.4	23.4		43.0	19.3		55.5	13.8		44.8	10.6	
4	6	32.4	28.6	0.335	30.9	28.4	0.639	29.4	23.3	0.262	41.6	25.5	0.181	47.5	16.1	0.200
Multiple cancer																
0	33	38.3	22.1		26.2	23.9		43.9	20.8		51.1	18.5		48.8	14.2	
1	13	38.6	14.3	0.964	22.4	16.9	0.609	41.7	16.4	0.732	50.5	10.7	0.911	48.3	8.5	0.916

NBNC HBV/HCV-negative

normal liver tissue, irrespective of the methylation status (Fig. 3b). Conversely, although *SPDYA* was highly methylated in a majority of HCC cell lines, its expression was detectable in all cells, and most of the HCC lines exhibited greater *SPDYA* expression than did normal liver tissue (Fig. 3b). The above results suggest that *KLHL35* and *PAX5* are epigenetically silenced in HCC cells. Consistent with that idea, treating methylated cell lines with a DNA methyltransferase inhibitor, 5-aza-dC, restored the expression of *KLHL35* and *PAX5* (Fig. 3c). On the other hand, the expression of *PENK* and *SPDYA* does not appear to be affected by methylation.

Analysis of LINE-1 methylation and its association with gene hypermethylation

It was previously reported that LINE-1 is frequently hypomethylated in HCC, though most of those studies focused on HBV-positive tumors. Similarly, by using the bisulfite